Introduction to Laser Diode–Pumped Solid State Lasers

Tutorial Texts Series

- *Introduction to Laser Diode-Pumped Solid State Lasers*, Richard Scheps, Vol. TT53
- *Modulation Transfer Function in Optical and Electro-Optical Systems*, Glenn D. Boreman, Vol. TT52
- *Uncooled Thermal Imaging Arrays, Systems, and Applications*, Paul W. Kruse, Vol. TT51
- *Fundamentals of Antennas*, Christos G. Christodoulou and Parveen Wahid, Vol. TT50
- *The Basics of Spectroscopy*, David W. Ball, Vol. TT49
- *Optical Design Fundamentals for Infrared Systems, Second Edition*, Max J. Riedl, Vol. TT48
- *Resolution Enhancement Techniques in Optical Lithography*, Alfred Kwok-Kit Wong, Vol. TT47
- *Copper Interconnect Technology*, Christoph Steinbrüchel and Barry L. Chin, Vol. TT46
- *Optical Design for Visual Systems*, Bruce H. Walker, Vol. TT45
- *Fundamentals of Contamination Control*, Alan C. Tribble, Vol. TT44
- *Evolutionary Computation: Principles and Practice for Signal Processing*, David Fogel, Vol. TT43
- *Infrared Optics and Zoom Lenses,* Allen Mann, Vol. TT42
- *Introduction to Adaptive Optics,* Robert K. Tyson, Vol. TT41
- *Fractal and Wavelet Image Compression Techniques,* Stephen Welstead, Vol. TT40
- *Analysis of Sampled Imaging Systems,* R. H. Vollmerhausen and R. G. Driggers, Vol. TT39
- *Tissue Optics: Light Scattering Methods and Instruments for Medical Diagnosis*, Valery Tuchin, Vol. TT38
- *Fundamentos de Electro-Óptica para Ingenieros,* Glenn D. Boreman, translated by Javier Alda, Vol. TT37
- *Infrared Design Examples,* William L. Wolfe, Vol. TT36
- *Sensor and Data Fusion Concepts and Applications, Second Edition*, L. A. Klein, Vol. TT35
- *Practical Applications of Infrared Thermal Sensing and Imaging Equipment, Second Edition*, Herbert Kaplan, Vol. TT34
- *Fundamentals of Machine Vision*, Harley R. Myler, Vol. TT33
- *Design and Mounting of Prisms and Small Mirrors in Optical Instruments*, Paul R. Yoder, Jr., Vol. TT32
- *Basic Electro-Optics for Electrical Engineers,* Glenn D. Boreman, Vol. TT31
- *Optical Engineering Fundamentals,* Bruce H. Walker, Vol. TT30
- *Introduction to Radiometry,* William L. Wolfe, Vol. TT29
- *Lithography Process Control,* Harry J. Levinson, Vol. TT28
- *An Introduction to Interpretation of Graphic Images,* Sergey Ablameyko, Vol. TT27
- *Thermal Infrared Characterization of Ground Targets and Backgrounds,* P. Jacobs, Vol. TT26
- *Introduction to Imaging Spectrometers,* William L. Wolfe, Vol. TT25
- *Introduction to Infrared System Design,* William L. Wolfe, Vol. TT24
- *Introduction to Computer-based Imaging Systems,* D. Sinha, E. R. Dougherty, Vol. TT23
- *Optical Communication Receiver Design,* Stephen B. Alexander, Vol. TT22
- *Mounting Lenses in Optical Instruments,* Paul R. Yoder, Jr., Vol. TT21
- *Optical Design Fundamentals for Infrared Systems,* Max J. Riedl, Vol. TT20
- *An Introduction to Real-Time Imaging,* Edward R. Dougherty, Phillip A. Laplante, Vol. TT19
- *Introduction to Wavefront Sensors,* Joseph M. Geary, Vol. TT18
- *Integration of Lasers and Fiber Optics into Robotic Systems,* J. A. Marszalec, E. A. Marszalec, Vol. TT17
- *An Introduction to Nonlinear Image Processing,* E. R. Dougherty, J. Astola, Vol. TT16
- *Introduction to Optical Testing,* Joseph M. Geary, Vol. TT15
- *Image Formation in Low-Voltage Scanning Electron Microscopy,* L. Reimer, Vol. TT12
- *Diazonaphthoquinone-based Resists,* Ralph Dammel, Vol. TT11
- *Infrared Window and Dome Materials,* Daniel C. Harris, Vol. TT10
- *An Introduction to Morphological Image Processing,* Edward R. Dougherty, Vol. TT9
- *An Introduction to Optics in Computers,* Henri H. Arsenault, Yunlong Sheng, Vol. TT8
- *Digital Image Compression Techniques,* Majid Rabbani, Paul W. Jones, Vol. TT7
- *Aberration Theory Made Simple,* Virendra N. Mahajan, Vol. TT6
- *Single-Frequency Semiconductor Lasers,* Jens Buus, Vol. TT5

Introduction to
Laser Diode–Pumped Solid State Lasers

Richard Scheps

Tutorial Texts in Optical Engineering
Volume TT53

Arthur R. Weeks, Jr., Series Editor
Invivo Research Inc. and University of Central Florida

SPIE PRESS
A Publication of SPIE—The International Society for Optical Engineering
Bellingham, Washington USA

Library of Congress Cataloging-in-Publication Data

Scheps, Richard, 1946–
Introduction to laser diode-pumped solid state lasers / Richard Scheps.
p. cm. – (SPIE Tutorial texts series ; v. TT53)
Includes bibliographical references and index.
ISBN 0-8194-4274-7 (pbk.)
1. Solid-state lasers 2. Diodes, semiconductor. I. Title. II. Tutorial texts in optical engineering ; vol. TT 53.

TA1705 .S42 2001
621.36'61—dc21 2001049384

Published by

SPIE—The International Society for Optical Engineering
P.O. Box 10
Bellingham, Washington 98227-0010 USA
Phone: (1) 360.676.3290
Fax: (1) 360.647.1445
Email: spie@spie.org
Web: www.spie.org

PDF ISBN: 9781510612792

Printed in the United States of America.

Introduction to the Series

The Tutorial Texts series was initiated in 1989 as a way to make the material presented in SPIE short courses available to those who couldn't attend and to provide a reference book for those who could. Typically, short course notes are developed with the thought in mind that supporting material will be presented verbally to complement the notes, which are generally written in summary form, highlight key technical topics, and are not intended as stand-alone documents. Additionally, the figures, tables, and other graphically formatted information included with the notes require further explanation given in the instructor's lecture. As stand-alone documents, short course notes do not generally serve the student or reader well.

Many of the Tutorial Texts have thus started as short course notes subsequently expanded into books. The goal of the series is to provide readers with books that cover focused technical interest areas in a tutorial fashion. What separates the books in this series from other technical monographs and textbooks is the way in which the material is presented. Keeping in mind the tutorial nature of the series, many of the topics presented in these texts are followed by detailed examples that further explain the concepts presented. Many pictures and illustrations are included with each text, and where appropriate tabular reference data are also included.

To date, the texts published in this series have encompassed a wide range of topics, from geometrical optics to optical detectors to image processing. Each proposal is evaluated to determine the relevance of the proposed topic. This initial reviewing process has been very helpful to authors in identifying, early in the writing process, the need for additional material or other changes in approach that serve to strengthen the text. Once a manuscript is completed, it is peer reviewed to ensure that chapters communicate accurately the essential ingredients of the processes and technologies under discussion.

The Tutorial Text series, which now numbers more than fifty titles, has expanded to include not only texts developed by short course instructors but also those written by other topic experts. It is my goal to maintain the style and quality of books in the series, and to further expand the topic areas to include emerging as well as mature subjects in optics, photonics, and imaging.

Arthur R. Weeks, Jr.
Invivo Research Inc. and University of Central Florida

"When we walked in fields of gold…"

–Sting

Contents

Preface

This book arose from a series of courses I presented on laser diode pumping. It covers a wide range of material, from the basics of laser resonators to advanced topics in laser diode pumping. The subject matter is presented in descriptive terms that will be understandable to the technical professional who does not have a strong foundation in fundamental laser optics. For the scientist or engineer with a more extensive background in laser design, the range and depth of the topics covered will provide a new and hopefully helpful perspective on development in this highly active area.

By presenting the material in courses to students from diverse backgrounds I have received numerous constructive comments that have been incorporated into the text. The modifications have enhanced the continuity of the technical material. As a result, this Tutorial Text represents an evolution from interactive classroom teaching to self-directed learning. I trust that the information presented will prove useful for those interested in diode pumping.

As the text is tutorial in nature, I have chosen not to include a comprehensive list of references. I have included a few general references and have cited papers that describe certain techniques in more detail than could be included in this book. In general, however, I have not provided the type of reference listing that one might expect in a review article on this subject and have therefore not been able to acknowledge much of the high-quality research that has been produced in this area over the past several decades.

Some of the material will become dated over time. The basic information presented in this book of course will not be affected by future developments, but for laser diodes the quoted costs and maximum output power levels will change. However, conclusions that are based on current (November 2000) numbers are readily modified when the relevant factors change. The book is generally explicit in terms of how these conclusions are reached, and the reader should have no problem including updated cost data using the paradigm provided in the text.

I want to end this section by thanking SPIE for offering me the opportunity to publish this book, and particularly Rick Hermann for helping overcome many of the difficulties that presented themselves. I also want to thank my family for their advice and support, my friends in France and the UK who made an important difference in my life, and my scientific colleagues, especially Joe Myers, who helped with the development of the concepts presented in the text.

Richard Scheps
San Diego, California

List of Symbols

A partial list of symbols used in the text:

α = absorption coefficient
α_m = maximum acceptance angle for TIR
η = wall plug efficiency
η_p = pump efficiency
θ = divergence half angle
λ = optical wavelength
ℓ = laser crystal length
σ' = effective stimulated emission cross section
σ_{em} = stimulated emission cross section
τ_c= cavity lifetime
τ_f = fluorescence lifetime
ν_p = frequency of pump radiation
$\Delta\nu$ = separation between longitudinal mode frequencies
AO = acousto-optic
A_m = resonator mode area
A_p = pump mode area
AR = anti-reflective
ASE = amplified spontaneous emission
c = speed of light
cw = continuous-wave
dn/dt = change in refractive index with temperature
ESD = electrostatic discharge
f = focal length
f_{mnq} = resonator optical frequency, where n and m reference the transverse mode
f_r = relaxation frequency
f_2 = fraction of ${}^4F_{3/2}$ population in the R_2 upper laser level
g_o = small signal (unsaturated) gain
g_n = resonator parameter for the n^{th} mirror, useful for determining mode stability
HR = highly reflective
HT = highly transmissive
I = pump intensity
I_{sat} = saturation intensity
K= thermal conductivity
L = resonator length
L_p = resonator round-trip passive loss, including output coupling
L_r =round-trip passive loss, excluding output coupling
L_s =single-pass passive loss

MOCVD= metal organic chemical vapor deposition, a process for manufacturing laser diodes
MTBF = mean time between failure
n^* = upper laser level population
n_i = average refractive index along the optical path within the laser resonator
n_m = refractive index of the m^{th} optical component
n_o = dopant density
NA = numerical aperture
P = absorbed pump power
P' = excitation pump rate
P_e = excess energy, i.e., the pump power less the threshold pump power
P_h = fraction of pump power deposited as heat
P_th = threshold pump power
PBC = polarization beamsplitter cube
PFN = pulse-forming network
PPLN = periodically poled lithium niobate
ROC = radius of curvature
qcw = quasi-cw
R = reflectivity
R_n = radius of curvature of the n^{th} resonator mirror
SHG = second harmonic generation
SLM = single longitudinal mode
T = transmission of output coupler
T_opt = optimum output coupling
TEM_{nm} = transverse electric and magnetic mode n,m
TIR = total internal reflection
w_0 = resonator mode waist ($1/e$ amplitude point)
w_n = resonator spot size on mirror n
z_n = location of resonator mode waist with respect to mirror n

Part I

Fundamentals of Laser Diode Pumping

Chapter 1

Introduction

This Tutorial Text provides an introduction to the design and operation of efficient diode-pumped lasers. The key advantages as well as the limitations of diode pumping are described, and several different types of lasers are presented. The primary goal is to provide the reader with an understanding of the basic components involved in diode pumping.

The first part of the book reviews the fundamental design considerations for the laser resonator. Details of the operation and selection of pump laser diodes, diode pump optics, laser resonator configurations, and resonator modes are presented. A significant portion of the text, presented in Part II, centers on the design and performance analysis of a fundamental mode end-pumped laser. The selection criteria and design rationale for each component of the resonator and pump optics are discussed, and the efficiency factors that affect overall laser operation are presented in detail. This basic end-pumped design is an ideal vehicle for understanding how the many concepts involved in diode-pumped laser design play out in an actual operating device, as well as providing a platform for illustrating the diverse applications of this technology. This is covered in Part III of the book. Advanced topics such as power scaling and side-pumping are discussed, as are techniques for efficient diode pumping of gain media other than Nd:YAG, including Cr:LiSAF and laser dyes. In addition, acousto-optic (AO) *Q*-switched operation, intracavity second harmonic generation (SHG), and single-longitudinal-mode laser output are described.

The book is designed to provide the reader with a range of basic skills related to diode pumping. These include the ability to design a basic diode-pumped laser resonator and pump optics using any one of a wide range of gain media, evaluate the potential of a given diode-pumped laser design for meeting specific objectives, differentiate between the various commercially available diode-pumped lasers, distinguish the types of laser diodes used for pumping, and understand the range and scope of current research and development in diode-pumped lasers.

This book will be useful for scientists, engineers,and program managers whose professional activities are likely to include working with or developing diode-pumped lasers. It is suitable for those wishing to receive an in-depth introduction to the subject, and is relevant as well to laser professionals who desire an overview of this field presented at a relatively advanced level.

1.1 Advantages of diode pumping

A laser in its most basic form consists of a gain element contained within an optical resonator. To produce laser emission the gain element must be excited. Excitation may be provided by electrical discharge through a plasma as is used for argon ion lasers, or by optical radiation such as that provided by flashlamps. As many solid state (but not semiconductor!) laser gain media are electrical insulators, optical excitation is the most appropriate means of producing gain. Diode pumping represents a type of optical pumping and as such has certain features in common with other types of optical pumping, particularly laser pumping.

Traditionally, optical excitation is produced by flashlamps, continuous-wave (cw) lamps such as arc lamps or tungsten-halogen lamps, or by other lasers, either pulsed or cw. Laser pumping has numerous advantages compared to lamp pumping, including

- directionality of the pump optical fluence;
- potentially high spectral overlap of the pump emission with the absorption bands of the gain medium; and
- the ability to match the inversion profile created by the pump beam to the fundamental laser resonator mode volume in the gain medium.

Lasers used as optical pump sources include flashlamp-pumped solid state lasers such as Nd:YAG, and gas lasers such as the argon ion and to a lesser extent the krypton ion laser. However, the electrical-to-optical conversion efficiency (η_D) for these lasers is generally quite low. For example, a typical commercially available doubled Nd:YAG laser consumes approximately 2.7 kW [160 J to the flashlamp at a 60% pulse-forming network (PFN) electrical conversion efficiency at 10 Hz] to produce about 3.5 W of 532-nm output power (350 mJ at 10 Hz). The η_D for this laser is only 0.13%. Ion lasers are even worse. For example, a 20-W argon ion laser requires about 40 kW of electrical power, yielding 0.05% for η_D. For these types of lasers the large heat load must be cooled, tens of kilowatts of electrical power are consumed, and their size, weight, and volume prevent their use in numerous applications such as those that require portability.

In addition, operational lifetimes are limited as well. Flashlamps last for only a few times 10^7 shots, while ion laser plasma tubes must be replaced after a few thousand hours of use. Although replacement flashlamps are relatively inexpensive, the cost of a new ion laser plasma tube represents 30–50% of the original cost of the entire laser.

Laser diodes, on the other hand, possess many of the advantages of other laser pump sources but have none of the disadvantages:

- Laser diodes have high η_D, typically 30% for multiwatt lasers, with efficiencies as high as 85% being reported for certain low-power devices.
- Lifetimes are quite high, with the mean time between failures (MTBF) ranging from 10^8 to beyond 10^{10} pulses, depending on the operating

conditions. Continuous-wave diodes have a MTBF of 5,000 to 20,000 hours. Diode lifetimes can be improved dramatically by (a) operating the diode at no more than 90% of its maximum rated power, and (b) cooling the diode so that the junction temperature is 5 to 10 degrees below room temperature.

- Cooling requirements are reduced compared to traditional laser pump sources since the electrical efficiency of laser diodes is much higher. However, as will be seen in the following pages, the heat is generated in much smaller volumes both in the laser diode and the gain element. This generally requires special techniques for thermal management.
- Weight and volume are greatly reduced compared to conventional laser pumping. Not only are the laser pump sources small, but the laser resonator can be made small as well. In addition, the voltage required to run the laser diodes is approximately 2 V, enabling battery operation. The operating voltage required to operate most high-power Nd:YAG and argon ion lasers is 208 V and 480 V, respectively.

However, there are some disadvantages associated with using laser diodes as optical pump sources. These are the following:

- The cost. Diode costs range from about (US)$10/W for low-duty-cycle pulsed diodes in an array to as much as $400/W for cw lasers in a fiber-coupled array. Costs vary with the diode package type as well as the number of diodes ordered. A 20-W cw diode array on a “sub-mount” (not completely packaged) can be obtained for only a few hundred dollars, while a packaged, fiber-coupled array hermetically sealed and complete with a Peltier cooler (for thermal management) and a monitor photodiode (to regulate the diode output power) can cost $8000. Individual cw diodes presently cost several hundred dollars for a 1-W device. Since flashlamps cost approximately 5×10^{-4} \$/W, one would not use laser diodes in place of a flashlamp if cost were the determining factor. Two notes about cost: First, the amounts quoted above are for 808-nm AlGaAs laser diodes. Other wavelengths may have different costs. For example, a 0.5-W visible (red) laser diode costs $2000 to $3000, depending on the package. Second, the “cost per watt” for pulsed diodes is computed using the diode peak power. Since, in general, pulsed laser diodes operate in steady state or “quasi-cw” (qcw) mode, the output power waveform for a square drive pulse is square as well. The peak output power corresponds to the plateau so that, for example, a 1-W qcw laser diode emits 150 μJ in a 150-μs-long pulse. Quasi–continuous-wave operation occurs for diode output pulse widths greater than around 100 ns.
- Sensitivity to electro-static discharge (ESD) and electrical transients. A short electrical spike will permanently damage a diode, so care must be taken both in handling the device as well as in the design of the electrical drive circuit.

- The diode emission is not monochromatic, but generally has a bandwidth of 1 nm for high-power individual diodes and 2 to 4 nm for linear diode arrays.
- The output from a laser diode is not collimated but highly divergent, and for diode arrays it is multiaperture as well. This presents a challenge for effective pump optics design.

The advantages and limitations of diode pumping are discussed throughout the text.

Chapter 2

Basic Concepts

The concepts related to lasers and optical physics presented in this chapter are discussed in descriptive rather than analytical terms. Although much of the discussion is quite basic, it masks the complex and often elegant underlying mathematics. Such treatment has its limitations but is designed to provide the necessary insight to the reader with only a general background in optics. For an in-depth discussion of the subject matter there are several comprehensive texts on laser physics [See, for example, *Lasers* by A.E. Siegman, University Science Books, Mill Valley, (1986).]

2.1 Lasers

Lasers are devices that generate coherent optical radiation. The word "laser" is an acronym for "light amplification by stimulated emission of radiation." The laser is used in a variety of applications, and lasers have been demonstrated that incorporate an extraordinary range of gain elements, pumping methods, and resonator designs. The main characteristics of lasers, which determine the scope of applications, are coherence, directionality, monochromaticity, and intensity (brightness).

In order to achieve laser action, a device must contain a gain element located in an optical resonator. The gain element is referred to as the "laser material" or "gain medium" and is what produces amplification by stimulated emission. The laser itself is named for the gain element. For example, a "dye laser" uses a dye solution as the gain medium, while the gain element in an "Nd:YAG" laser is composed of trivalent neodymium ions doped in an yttrium aluminum garnet ("YAG") crystalline host.

The gain element is composed of a material that is able to support a population inversion when excited. A photon passing through a gain element has a higher probability of producing a second photon (at the same wavelength) by stimulated emission than it has of being absorbed. The requirements for producing a population inversion vary for different types of excitation techniques. In this book we are concerned only with optical excitation—more specifically, with laser diode pumping. Thus, we need to specify the optical pump conditions that enable the laser diode(s) to produce a population inversion.

A resonator is required for the generation of optical feedback. Without feedback the gain element provides optical amplification but not the directionality associated with laser emission. (Even when located within a resonator, however, the gain element may have sufficient single-pass gain to produce amplified spontaneous emission, or ASE). A gain element lacking feedback can be used as an optical amplifier for light from a low-power laser. However, in order to achieve laser action the gain element must have optical feedback.

An optical resonator consists of at least two mirrors aligned so that absent optical losses light remains trapped between the mirrors. (Strictly speaking, this is true only for stable resonators, as noted below). The spatial distribution of light within the resonator is described mathematically by Gaussian eigenmodes ("modes"). Resonator types and resonator modes are important concepts for producing efficient diode-pumped laser operation and will be discussed throughout this book. These concepts are presented in more detail below.

As an optical amplifier is composed of an active gain element without a resonator, one can also consider a resonator without a gain element. Fabry-Pérot interferometers are examples of the latter. The point of this discussion, however, is that it is not possible to produce a laser without an active gain element located within a properly aligned resonator.

2.2 Resonators

Laser resonators are open structures containing two or more mirrors that are aligned to produce optical feedback to the gain element. In the simplest case, a resonator consists of two aligned mirrors. These mirrors are called end mirrors and define the optical cavity. Optical radiation circulates within the cavity, bouncing back and forth between the end mirrors and passing through the gain element.

Resonators can be stable or unstable. Stability is determined by the radii of curvature of the mirrors, the spacing between the mirrors, and the refractive index of the material in the recirculating path. In a stable resonator the lowest-order modes remain close to the optical axis, and diffraction losses are small. Stimulated emission takes place only within a relatively slender volume in the gain element. Higher-order modes are required to extract all of the available power from the pumped volume when the pump light fills the rod. This is often the case with lamp-pumped solid state lasers. Other features of stable resonators will be described in the sections that follow. Unstable resonators, on the other hand, have mode volumes that are typically much larger. These resonators are characterized by large diffraction losses, and, in fact, the diffraction spread past one of the end mirrors may be used as an output coupling mechanism. Unstable resonators are particularly useful for high gain media such as certain gas or dye lasers, but stable resonators are more practical for diode-pumped lasers. As will be shown, the small volume for the lowest-order mode in a stable resonator is an important advantage for diode pumping, allowing the production of high-efficiency laser output with excellent transverse mode control. Therefore, in this book we will discuss only stable resonators.

There are numerous types of resonators that are commonly used to produce laser emission. Two that are frequently used for diode pumping are the hemispherical—or, more accurately, "nearly hemispherical"—resonator and the confocal resonator. The first type of resonator is composed of one flat and one concave mirror separated by the radius of curvature of the curved mirror. This resonator is illustrated in Fig.

2.1. The confocal resonator is composed of two curved mirrors. For the symmetric confocal resonator both mirrors have identical radii of curvature and the separation is equal to the mirror radius. This resonator is illustrated in Fig. 2.2.

2.3 Laser resonator transverse modes

The distribution of light confined within an optical resonator is described by spatial patterns called transverse modes. Transverse modes are eigenmodes of the resonator. The Fresnel-Kirchoff formulation of Huygen's principle can be used to derive the integral equation that relates the fields at the two opposing mirrors of the cavity. Resonator modes are sets of transverse patterns that have the following property: after one round trip through the resonator, the exact pattern returns to the same location. These self-reproducing sets of intensity patterns represent the transverse modes of the resonator. The modes are approximately plane waves multiplied by the

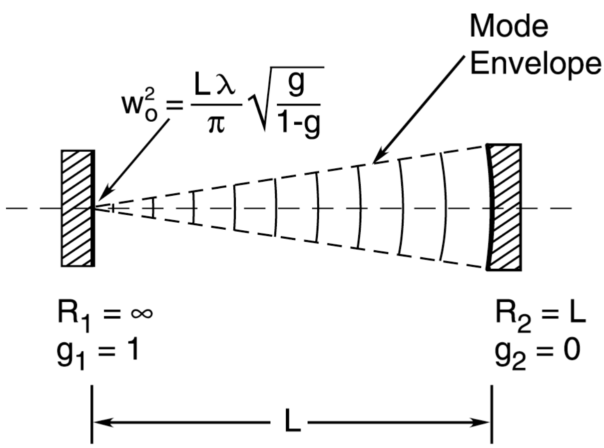

Figure 2.1. Hemispherical resonator.

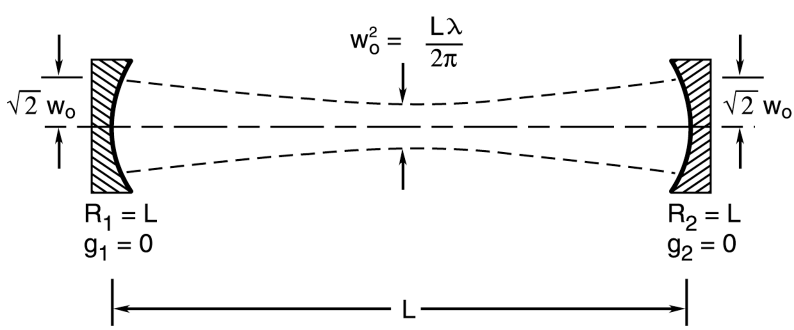

Figure 2.2. Symmetric confocal resonator.

transverse amplitude and phase profiles for the given eigenmode. These modes are referred to as TEM_{nm} for transverse electric and magnetic, and they are determined by the mathematical solution to the eigenequation for the resonator.

The transverse mode patterns will in general have a different field pattern at each transverse plane within the resonator. Therefore, the shape of the mode changes as it propagates along the resonator axis. The intensity profile of the transverse patterns is Gaussian, and the transverse modes are sometimes referred to as Hermite-Gaussian modes. The *n* and *m* subscripts in the TEM_{nm} mode designator refer to the number of intensity nodes of the resonator mode pattern along the x and y axis, respectively. That is, in rectangular coordinates, the x and y axes are orthogonal to each other and to the resonator propagation, or z, axis. Several mode patterns are illustrated in Fig. 2.3.

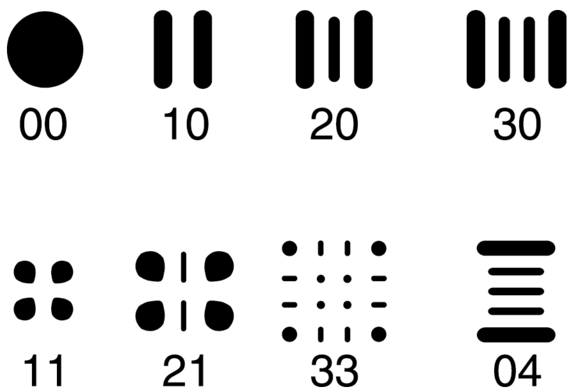

Figure 2.3. Transverse Gaussian mode patterns with *n, m* indicated.

2.3.1 TEM_{00}

The TEM_{00} mode is the lowest-order transverse mode. It has the lowest threshold, smallest beam waist and divergence, and contains no nodes in the output beam transverse intensity distribution. In discussing laser beam parameters such as mode waist and divergence throughout this text, it is implicit that the laser is operating in the TEM_{00} mode. There are several resonator mode parameters that are useful for discussing modes in general, and these are shown in Fig. 2.4. One important parameter is the mode waist w_0, which refers to the minimum cross-sectional beam radius within the laser resonator. The cross-sectional beam radii or "spot sizes" at the two end mirrors are labeled w_1 and w_2, respectively. The location of the waist relative to each mirror is designated as z_1 and z_2, respectively, while the separation of the mirrors is labeled L.

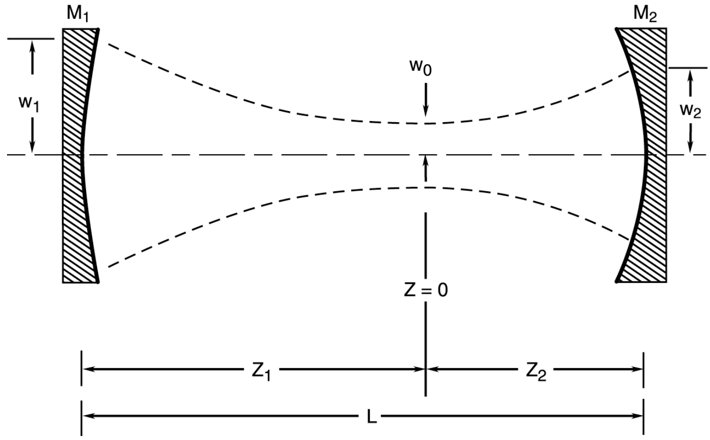

Figure 2.4. Notation for a two-mirror cavity.

The larger the spot sizes w_1 and w_2 relative to the mirror diameter, the larger the diffraction loss. For the exactly hemispherical resonator the spot size is infinite at the curved mirror and the waist vanishes at the flat mirror. The infinite spot size at the curved mirror makes the resonator unworkable. Therefore, in practice, the separation between the two mirrors is shortened slightly to produce a "nearly hemispherical" resonator. In this resonator the spot sizes at both mirrors are finite, and the beam waist remains at the flat mirror. The waist and spot size at the flat and curved mirrors are determined by

$$w_0^2 = w_1^2 = \frac{L\lambda}{\pi}\sqrt{\frac{g_2}{g_1(1-g_1g_2)}} \tag{2.1}$$

and

$$w_2^2 = \frac{L\lambda}{\pi}\sqrt{\frac{g_1}{g_2(1-g_1g_2)}}\,, \tag{2.2}$$

respectively, where

$$g_1 = 1 - L/R_1 \text{ and } g_2 = 1 - L/R_2 \tag{2.3}$$

and R_1 and R_2 are the radii of curvature of the flat and concave mirrors, respectively.

For the symmetric confocal resonator, the beam waist is located midway between the two mirrors. The waist and beam spot sizes at the two mirrors are

$$w_0^2 = L\lambda/2\pi \tag{2.4a}$$

and

$$w_1^2 = w_2^2 = 2w_0^2. \tag{2.4b}$$

Why do we care about the resonator mode size and location? This information specifies the volume within the gain element from which energy is extracted ("active volume"). Pump light deposited outside the mode volume is wasted. In some cases, putting too much excitation outside the boundaries determined by the lowest order or fundamental mode (TEM_{00}) can provide higher-order transverse mode operation in the laser. In order to produce an efficient TEM_{00} diode-pumped laser, it is important to tailor the pump energy deposition profile to fit within the active volume.

2.3.2 Multimode operation

Higher-order modes are less efficient and have a higher threshold, but will oscillate nonetheless if care is not taken in the resonator and pump optics design. Misalignment of the end mirrors can produce a single, higher-order transverse mode. However, in cases where too much pump energy is deposited in a relatively large volume, more than one transverse mode oscillates simultaneously. This is termed multimode operation and is routinely produced in many commercial lamp-pumped high-power lasers. The output beam characteristics in multimode operation, such as the divergence, focused spot size, Rayleigh range, etc., are poorly characterized. On the other hand, multimode operation can produce high laser output power in a side-pumped geometry, and for that reason it is common for lamp-pumped lasers.

2.3.3 Advantages of single transverse mode operation

TEM_{00} mode operation has numerous advantages that make it a desirable design goal. For example, the beam divergence is low, which provides high power density over large propagation distances. The focused spot size is smaller than that produced by higher-order modes and contains no nodes, making this type of beam useful for laser drilling, medical treatment, and other applications that require high brightness and small spot sizes. In addition, because the output beam intensity is characterized by a uniform Gaussian profile, it is useful for many illumination and imaging applications.

TEM_{00} operation is a particularly important consideration for efficient diode pumping. The resonator mode waist is the smallest of all transverse modes, therefore providing the opportunity for an excellent match to the tightly focused pump beam in an end-pumped geometry. The mode volume is small as well, so that for either side pumping or end pumping the diode pump flux can be concentrated within the laser resonator mode to produce high pump power density. This allows high gain to be developed within the resonator, and produces high pump optical-to-laser output efficiencies.

2.3.4 Longitudinal modes

Standing-wave resonators exhibit interference, and as a consequence, laser resonators support only specific optical frequencies. The separation $\Delta\nu$ between adjacent frequencies is given by

$$\Delta\nu = c/2n_i L, \tag{2.5}$$

where n_i is the average refractive index along the optical path within the laser cavity. When a laser produces output at only one of the supported optical frequencies, it is said to be operating "single frequency." There are many interesting applications for single-frequency laser operation, and two types of single-frequency lasers will be discussed in this book. One is the single-mode laser diode, which generates a single transverse as well as single longitudinal mode. These diodes are useful for certain types of end pumping and are discussed below. The other is a diode-pumped single-frequency laser. These lasers have many applications, including laser gyros and production of efficient nonlinear optical conversion, which will be discussed in more detail in Part III of this book.

When referring to longitudinal modes, the transverse mode designator includes a third subscript "q" and is written as TEM_{mnq}. These subscripts describe the transverse intensity and phase properties of the resonator mode (m, n) as well as the mode optical frequency (q). The optical frequency depends on the value of m and n as well as q, and is given by

$$f_{mnq} = \left[q + (m+n+1)\frac{\cos^{-1}\sqrt{g_1 g_2}}{\pi} \right] \frac{c}{2n_i L}, \tag{2.6}$$

where the factor g_n is given by

$$g_n = 1 - L/R_n, \tag{2.7}$$

and R_n is the radius of curvature of the n^{th} end mirror.

2.4 Laser diodes for pumping solid state lasers

Modern laser diodes are manufactured with a wide variety of architectures, packages, and power levels. We will limit the discussion of laser diodes in this book to those that are used for optical pumping. In this section we will consider only AlGaAs laser diodes, as other semiconductor lasers will be discussed in Part III.

AlGaAs diodes can be designed to emit at a wavelength in the range of approximately 725 nm to 850 nm. The emission wavelength is determined by the ratio of Al to Ga in the active region. The higher the Al concentration, the shorter the output wavelength. Since the market for high-power lasers is driven by pumping Nd-doped materials, the vast majority of diodes sold for laser pumping produce emission in the 808- to 810-nm range.

A heterojunction diode is shown schematically in Fig. 2.5. Semiconductor lasers operate by passing current through a p-n junction. Electrons traveling in the n region must have more energy than those traveling in the p region. Therefore, when the electron from the n region passes into the p region, it has excess energy. This excess energy is lost by photon emission. Light-emitting diodes (LEDs) operate on this same principle. The feature that distinguishes laser diodes from LEDs is that the density of energetic electrons located in the p region is sufficient to produce stimulated emission. As in a traditional laser, the gain medium is contained within a laser resonator. However, in the case of laser diodes, the resonator mirrors are the end faces of the semiconductor chip itself.

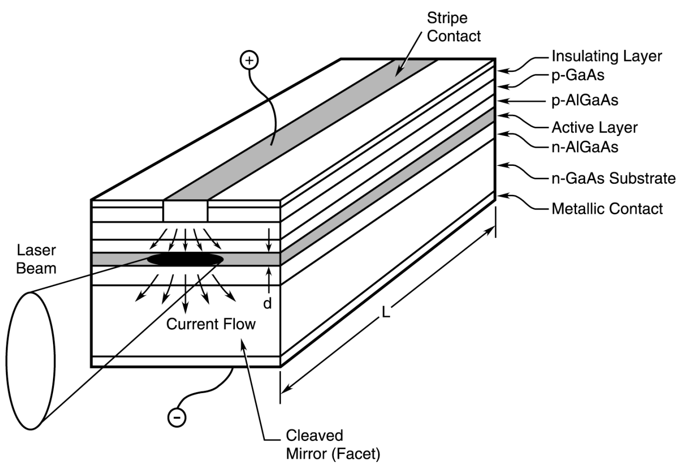

Figure 2.5. Schematic of a gain-guided heterojunction laser.

Several terms that are used to discuss the various features of laser diodes are worth reviewing. Referring to Fig. 2.5, the region of the structure that produces the gain is called the "active layer" or "active region." The Al content in this layer determines the output wavelength, and as shown, light emitted from the laser is produced in this layer. The laser resonator is composed of two flat end mirrors. These mirrors are formed by cleaving the end faces (called "facets") of the semiconductor device. The faces may be coated to produce a desired reflectivity, or may be provided with a "passivation" coating to protect the facets from damage or contamination by trace pollutants in the air. The high refractive index of AlGaAs produces 30% reflectivity per (uncoated) facet, generating sufficient feedback for efficient laser diode output. Since a laser diode emits light through both facets, high-power diodes are typically coated HR (highly reflective) on the rear facet. The electrical current that flows to the junction enters the device at a "stripe" contact. This contact runs the entire length of the diode, and individual diodes, whether discrete or one of many contained in a diode array, are referred to as single-stripe diodes.

2.4.1 Single-stripe diodes

Most high-power diodes are "gain guided," which means that horizontal confinement of the light flux propagating through the active region is accomplished by the small refractive index variation produced by the current-generated population inversion. If the light spreads in the horizontal plane outside of the horizontal dimensions of the stripe or "stripe width" (typically between 1 μm and 200 μm), it will be absorbed by the unexcited region of the active layer. In the vertical direction the lower refractive indices of the surrounding n and p layers ("cladding layers") reflect light from the interface back into the active region. Since the horizontal waveguiding produced by the gain is a function of the excitation current levels, poor mode control results from these types of devices. Index-guided laser diodes have structural components incorporated into the architecture to confine light in the horizontal plane. These devices produce beams with much higher beam quality, but are typically limited in power to only a few hundred milliwatts.

2.4.2 Single-mode diodes

Single-mode diodes produce output in a single longitudinal as well as transverse mode. The highest power produced by a commercial single-mode AlGaAs diode is 200 mW. The advantage of the single-mode diode for laser pumping is that an extremely small focused pump spot size can be obtained. The spatial properties of the diode output beam are excellent as well. Furthermore, the output wavelength of the single-mode laser can be tuned (over several nanometers) to match the center of an absorption line in the solid state laser crystal. This allows high-density pump power deposition. Wavelength tuning is accomplished by changing the junction temperature; the laser output wavelength increases at the rate of +0.3 nm/°C. Temperature tuning to the absorption peak combined with the high beam quality produces low-threshold, high-slope-efficiency laser operation. Single-mode diodes cost significantly more per watt but are useful for pumping compact, low-power lasers.

2.4.3 Pulsed and cw diode operation

Individual laser diodes are inherently cw devices. Under qcw operation, the steady-state diode output characteristics are essentially cw and the peak output power produced by a single-stripe diode is limited to the maximum cw output power. For high-power linear or two-dimensional diode arrays, the cooling efficiency determines the maximum device duty factor. The duty factor represents the percentage of laser diode "on time." For example, a linear array with a 20% duty factor indicates that the pulse width cannot exceed 20% of the inverse of the pulse repetition frequency. This would limit such an array producing 100-μs pulses to a repetition rate of 2 kHz.

Heat generated in the p-n junction must be removed rapidly to allow diode operation, with the heat load becoming more severe as the duty factor increases. Due to the low thermal conductivity of the semiconductor substrate, even the most advanced diode package designs have a limited cooling capacity. This limits the packing density of stripes on a cw array to about one-half the packing density of a low-duty-factor qcw array.

2.4.4 Diode manufacturing terms

There are several methods that are used to produce laser diodes. The most common process is metal-organic chemical vapor deposition (MOCVD). The manufacturing process of depositing layers with the desired III-V elemental composition and thickness on a heated GaAs substrate is called "epitaxy." Epitaxial growth occurs on a GaAs substrate in the form of a thin disk or "wafer," typically 5 to 10 cm in diameter. Since the diode optical cavities are generally several hundred microns long, large numbers of diodes can be manufactured on a single wafer. The finished wafer is cleaved or "diced" into individual lasers or linear arrays. Cleaving produces the facets that serve as the end mirrors of the laser. Cleaving is effective because the GaAs fractures readily along certain well-defined crystal planes.

The lasers are soldered onto a copper heat sink, which also acts as the electrical ground. The other side of the diode contains an electrical lead that is attached or "wire bonded." High-power diodes are manufactured with the p side down for better thermal management, so that the wire-bonded lead requires a negative voltage. Single-stripe diodes may be sold in open packages, which consist of a copper mounting plate that serves as the ground and a wire tang to connect the negative electrical lead. Hermetically sealed packages are also available for these diodes, with TO3 and 9-mm "cans" representing the most common package types. Some laser packages include a photodiode to monitor the laser output power. Other packages include a thermoelectric or "TE" cooler to remove heat from the diode and to regulate the junction temperature.

2.4.5 Laser diode arrays

Laser diode arrays are linear arrays of single-stripe diodes manufactured on a continuous GaAs substrate. Arrays can be either phased or incoherent, although phased arrays are uncommon and are of interest primarily for their historical significance. In the mid-1980s the highest-power laser diodes were produced as phased arrays, consisting of 10 or so stripes spanning a total width* of about 200 μm. The regions between each stripe were unexcited and therefore absorbing. Historically, the concern was that if a single wide stripe were used, photon paths transverse to the laser axis would generate sufficient ASE to produce inefficient operation. Power output ranged from 100 mW to 1 W. The spacing between the stripes was small enough so that cross communication between adjacent stripes produced coupled operation. However, each stripe operated 180° out of phase with respect to the adjacent diode, leading to a twin-lobed far-field pattern. Nonetheless, the output power and focusing characteristics of these lasers were adequate to produce high optical conversion efficiency for diode pumping.

---

*In traditional semiconductor processing terminology, the dimension "width" refers to the separation of the laser end mirrors, while "length" indicates the transverse span of the stripe. In this book, the terms length and width designate the dimension of the laser along, and transverse to, the optical axis, respectively. This reflects traditional laser terminology.

Eventually, manufacturers were able to replace the individual emitters with a single- wide-stripe diode that produced the same output power and far-field spatial patterns. Research continued, and wide-stripe lasers emitting 3 to 5 W are currently available. The term "wide" is referenced to the stripe length and generally refers to stripe widths between 50 μm and 500 μm. Phased arrays are no longer manufactured for the consumer market.

In the course of producing wide-stripe diodes, manufacturers began to sell 1-cm-wide "bars," which are incoherent linear arrays of 1-W single-stripe diodes. In this type of array, each stripe operates independently (phase and wavelength) relative to the other stripes on the bar. Ten 1-W stripes were sold as a 10-W linear array. At first these were only available for quasi-cw operation with a 1% duty factor, but semiconductor packaging and processing technology have progressed rapidly over the past several years. Currently, up to 100 W per 1-cm bar is sold with a 1% duty factor for about $1000 in small quantities. Higher duty factors are available at reduced output power. Linear arrays that produce up to 65 W cw are also available. By vertically "stacking" quasi-cw linear arrays, manufacturers can produce 2D arrays. A stack of 25×100-W bars can be assembled to produce a $1\times1\ \text{cm}^2$ array with a qcw output power of 2500 W. The maximum power currently available from a 2D array is 5 kW.

2.4.6 Laser diode beam spatial properties

Laser diode beam spatial properties are unlike those associated with most conventional lasers, and they are illustrated schematically in Fig. 2.6. In the plane of the junction the beam divergence is low, typically 10° FWHM, but is many times diffraction limited. As a consequence, a diffraction-limited focused spot cannot be achieved in this plane, and lower-than-optimum pump power density is produced in the gain element. On the other hand, divergence in the plane perpendicular to the junction is much higher, typically 35° to 40° FWHM, but is diffraction limited. In

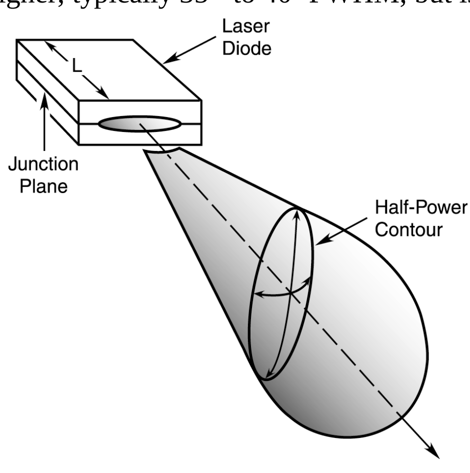

Figure 2.6. The shape of the output beam from a laser diode.

this plane it is possible to achieve high pump power density with a diffraction-limited spot size.

The unique spatial properties of the diode output beam requires collimating pump optics with special characteristics. First, a short-focal-length, high-numerical-aperture (NA) lens is required to collect the light in the transverse plane. Second, the different divergences in the two orthogonal planes requires anamorphic optics—that is, optics with different focusing properties in the two planes. Third, there is astigmatism in the diode output due to the two different divergences. Even when perfectly collimated, the diode output beam will be elliptical, so in some cases circularization using anamorphic prism pairs may be desirable. And finally, for linear or 2D arrays, collimating and focusing is further complicated by the fact that the optical source is an incoherent array of divergent beams. The issues related to the design of the pump optics will be discussed in more depth in Part II.

2.5 Optical fiber concepts

Optical fibers are waveguides that consist of a core or central region surrounded by a cladding. The cladding has a lower refractive index and confines the light in the core by total internal reflection (TIR). Since fiber-coupled diodes and diode arrays are useful for end pumping, we will briefly review two fiber optic concepts.

2.5.1 Numerical aperture

The NA of a fiber is a measure of the maximum angle for TIR in the waveguide. The higher the NA, the greater the maximum angle. The fiber NA affects the input coupling optics selection as well as generally determining the cone of light emerging from the fiber. The NA can be determined simply from Snell's law and trigonometry, and it is given by

$$\mathrm{NA} = n_0 \sin\alpha_\mathrm{m} = n_1\left[1-\left(\frac{n_2}{n_1}\right)^2\right]^{\frac{1}{2}}, \tag{2.8}$$

where n_0, n_1, and n_2 are the refractive indices of air, the fiber core, and the fiber cladding, respectively, and α_m is the maximum angle of incidence for TIR. The fiber geometry is shown schematically in Fig. 2.7. For an object at infinity, the *f* number of a lens is related to its NA by

$$\mathrm{NA} = 0.5/(f\ \text{number}). \tag{2.9}$$

2.5.2 Core size

An optical fiber is illustrated in Fig. 2.8. The fiber architecture consists of a central core surrounded by a concentric cladding with an approximately 1% lower refractive index. Fibers are typically composed of fused silica. A protective coating of cushioning material such as acrylate may surround the cladding. Fibers used to couple the output of a high-power single-stripe laser generally have large core diameters—50 to 100 μm or more. These types of fibers are called "multimode fibers," as they support more than one guided mode or optical path through the fiber core.

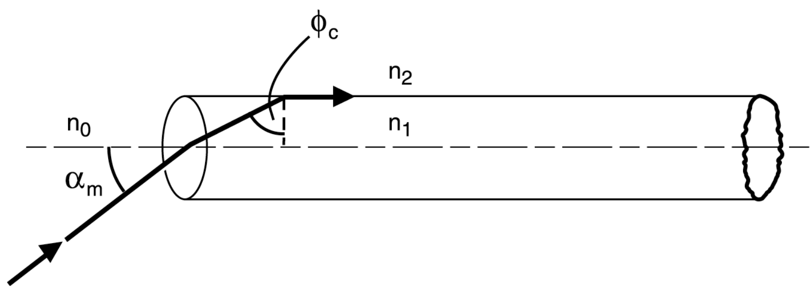

Figure 2.7. Ray geometry for the determination of fiber NA.

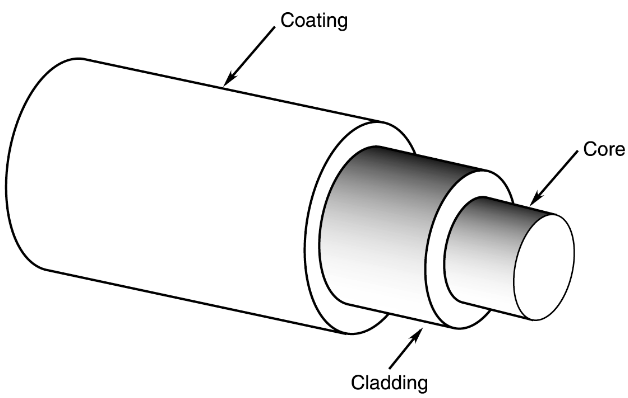

Figure 2.8. Optical fiber.

2.5.3 Fiber-coupled single-stripe diodes: Advantages

Many high-power commercial end-pumped lasers incorporate fiber coupling due to the numerous advantages of this technique for diode-pumped lasers. These are the following:

- The heat generated by the diodes can be more readily removed if the diodes are not contained near the laser head.
- The laser head can be made more compact if the diodes and the associated electronics are located in a separate, remote package.
- If a diode fails it can be replaced more readily. The diode package, typically located inside the laser control electronics box, is replaced with the new

diode and the fiber is subsequently connected using a standard connector. The laser head need not be opened.
- Alignment is far simpler and more forgiving. Unlike discrete optics, where alignment along as many as five separate axes for each lens (three translation, two tilt) is often critical for good coupling, the larger pump spot size and lower NA associated with fiber coupling allow for more flexible, lower tolerance alignment. This facilitates more stable operation at high laser output power.

There are a few disadvantages as well:

- Fiber-coupled diodes provide less pump power because of optical coupling losses. For example, a 1-W diode produces about 800 mW through a fiber.
- The diodes are more expensive to replace when they fail. Fiber coupling is labor intensive, adding to their manufacturing cost.
- Fiber-coupled diodes are less-efficient optical pumps due to the lower pump power density. In general, it is not possible to produce as small a pump spot from a fiber-coupled diode as from a diode imaged with high-NA discrete optics. Reducing the pump image in the crystal requires demagnification, which in turn increases the pump divergence. This lowers the pump efficiency, as will be discussed in more detail in Part II.

2.5.4 Fiber-coupled laser diode arrays

The production of higher-output-power end-pumped lasers requires higher diode pump power in a format compatible with the end-pumped geometry. While power scaling will be addressed in more detail in Part III, one means for providing increased pump power is through a fiber-coupled diode array. In this type of device, a 1D cw diode array is configured with each individual stripe connected to an optical fiber. The array of fibers is "bundled" so that the pump power is optically similar to that conducted through a single larger core fiber.

2.5.4.1 Bundled fibers

Fiber bundles are available in different diameters. The smaller the effective fiber bundle core, the higher the pump brightness and therefore the better the pump efficiency.[*] A commonly available fiber-coupled array starts with a 20-W cw bar. The fiber bundle diameter is 600 μm and the fiber NA is 0.37. The coupling efficiency of diode output-to-waveguided emission is 80%, so that the fiber delivers 16 W of usable pump power. The major limitation for fiber-bundled diode arrays is cost. As mentioned previously, the fiber coupling process is labor intensive. For example, the current price (in low quantities) for a fiber-coupled 16-W diode array (compete with integrated cooler and monitor diode) is about $8000, compared to

[*] This assumes that the increased thermal load can be dissipated efficiently.

about $2000 for the 20-W cw diode bar. While these prices will decline in time, one can expect that a fiber-coupled array will continue to add substantial value to the total price.

2.6 Light ducts

Light ducts or lens ducts are alternatives to fibers. A lens duct is illustrated schematically in Fig. 2.9. Ducts are available commercially and can be thought of as a "light funnel." Developed for 2D arrays, where light is concentrated in both the vertical and horizontal planes, light ducts condense and homogenize the output of a diode array. Lensing occurs at the curved input face, and ducting is accomplished by TIR within the interior of the guide. The pump beam emerges from the small output face of the duct, taking on the exit face dimensions. The duct can be manufactured with the exit face in the shape of a spherical or cylindrical lens to further condense the diode array emission.

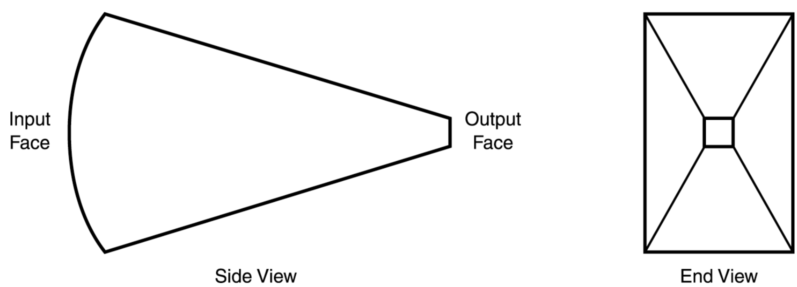

Figure 2.9. Commercial light ducts.

For end pumping, the duct can be used in conjunction with a 20-W cw array. The throughput is somewhat higher than fibers, allowing the duct to deliver approximately 18 W to the rod. The primary advantages of the duct are ease of use and overall cost. Unlike fibers, alignment of the duct to the bar is a single process, independent of the number of individual stripes on the array. In addition, the cost of the diode bar is significantly lower, as noted above.

Part II

Basic End-pumped Laser Design

Chapter 3

Design of a TEM_{00} Continuous-Wave Diode-pumped Nd:YAG Laser

In this chapter we will go through in detail the steps required to design a basic diode-pumped cw Nd:YAG laser. The purpose of this exercise is to understand in a pragmatic sense the considerations and trade-offs that must be made in designing this type of laser. This process will also establish a framework for the discussion of the more advanced concepts that are presented in Part III. In some cases, the choice of a particular component will be obvious from the outset, and reading through the material that describes different considerations and design trade-offs may seem tedious. But the selection of each component is used in this section as an opportunity to present a more detailed view of the design process, component by component. It is not simply focused on the design of one specific laser.

The specifications for the laser we will design are given in Table 3.1.

Table 3.1. Laser design specifications.

Output power (W)	1
Wavelength (μm)	1.06
Polarization	none
Transverse mode	TEM_{00}

For any optically pumped laser the basic components are the same. To begin with, one needs a gain element that can become active (sustain a population inversion) when illuminated with light of a given frequency. Of course, the gain element must be contained within an optical resonator. In addition, one needs a pump source capable of providing sufficient intensity at the appropriate wavelength(s) to pump the gain element, and an optical relay system to transport the pump flux from the source to the gain element. The major components for a diode-pumped laser fit the generic paradigm, but the pump source is one or more laser diodes. The components are illustrated schematically in Fig. 3.1.

The structure of this section is mapped by the schematic shown in the figure, but in the following manner. First the gain element is selected. This determines the wavelength of the laser diodes, which are discussed next. Then, the several considerations relating to the resonator are presented, and the chapter concludes with a discussion of the pump optics. But, before any of this is presented, the pump configuration must be determined.

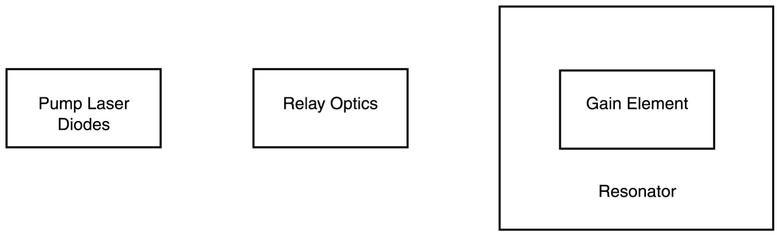

Figure 3.1. Functional diagram of the diode-pumped laser.

3.1 Considerations: End-pumped or side-pumped?

When beginning with an entirely new diode-pumped laser design, one of the first questions that arises is whether it is to be end-pumped or side-pumped. There are some simple guidelines that can aid the selection of the appropriate pump geometry, but the final decision should be made through evaluation of the advantages of each approach in terms of design priorities, such as electrical efficiency or component costs. These guidelines will be described in detail below, and a comprehensive review of the benefits and disadvantages of each pump technique will be provided.

Traditionally, solid state lasers have been optically excited using lamps. With lamp excitation the obvious choice for the pump geometry is side pumping. When high- power qcw diodes first became available, the side-pumped geometry was used to produce lasers that operated like flashlamp-pumped, *Q*-switched Nd:YAG. The decision to opt for side pumping was due in part to tradition, but was also a reflection of the diode array geometry. The 1-cm-long array can be oriented parallel to the optical axis of the laser rod and used with little or no imaging to illuminate the active region. On the other hand, diodes suitable for end pumping—that is, single-stripe or fiber-coupled diodes—are not available at the output power levels required to produce high-peak-power *Q*-switched laser operation. Note that for a desired output of 1 J per pulse at 1.06 μm, assuming a 35% pump diode-to-Nd:YAG output conversion efficiency and a 150-μs-long excitation pulse, the required laser diode output power is $(0.35\times1.5\times10^{-4})^{-1} = 19$ kW.

Therefore, one guideline is that if high output energy is desired, side pumping with multiple-diode arrays may be the appropriate choice. But how high is high? Perhaps we can determine a practical gauge based on diode array technology. The highest output power fiber-coupled diode array suitable for end pumping produces 40 W. Using two of these arrays to pump a Nd:YAG rod, and making the same assumptions as those at the end of the paragraph above, we would conclude that end pumping might only produce about 3 mJ per pulse.

However, as lens ducts allow 1D and 2D arrays to be used for end pumping, the higher-power qcw diodes that are associated with side-pumped lasers can be used for end pumping as well. The truly restrictive factor for power scaling is the high pump power density characteristic of end pumping. The power limitation for end pumping is therefore not so much one of the availability of suitable diodes as it is of thermal loading, thermal fracture, thermal birefringence, and to a varying degree, cost. The relative importance of these factors depends on the specific pump geometry, the resonator configuration, and the host crystal, which will be addressed in Part III.

High pump power density limits the end-pumped laser output power for both cw or qcw diode pumping, although the lower the pump diode duty factor, the lower the average thermal loading. However, for low-power operation, end pumping is almost always the better choice. This is because of the inherently high pump coupling efficiency, the low threshold power, and the high slope efficiency produced by the high pump power density. An additional advantage of end pumping is the natural selection of the TEM_{00} mode. And, of course, thermal issues are less important at low power.

These guidelines can be quantified to a certain extent based on average laser output power and mode of operation, although it is important to emphasize that these are guidelines and not rules. For cw operation with a desired output power under 1 W, end pumping is the best choice. In the 1-W to 10-W output power range, end pumping is often the better choice. However, side-pumping designs should be evaluated for comparison, particularly toward the high end of the range. Above 10 W, side pumping is generally superior to end pumping. For pulsed operation, the pump geometry considerations are somewhat more difficult to quantify; they depend on several factors, including the average power, duty factor, peak pump power, and resonator design. For low-average-power, low-peak-power pulsed operation, end pumping is still the best choice. On the other hand, pulsed or *Q*-switched lasers producing hundreds of millijoules per pulse, as well as those producing more than a few watts of average power, should be side pumped. These guidelines apply primarily to the 1-μm transition in Nd-doped lasers, and different criteria may be more appropriate for other gain media or other Nd laser wavelengths. For example, cw end-pumped Yb-doped lasers (discussed in Part III) have been demonstrated at power levels exceeding 1 kW.

Each pump geometry has specific advantages and disadvantages, which are listed below. As stated previously, only stable resonator configurations are discussed in this text, and the design criteria are specific to this type of resonator. The considerations can be different were one to address unstable resonators.

For end pumping, the advantages are

- High pump power density produces low-threshold, high-slope-efficiency operation.
- The pump geometry can create a "gain aperture" (explained later in this section) for naturally generating the TEM_{00} resonator mode.

- Rod lengths of 5 to 10 mm allow efficient absorption of the broad-spectral-bandwidth diode emission to produce high pump efficiency.
- Highest optical conversion efficiency and pump-coupling efficiency are available with this type of diode pumping, as the pump light can be deposited entirely within the fundamental mode volume.

The disadvantages are

- Power scaling is complicated by the single emission aperture requirement for the pump diode or diode array.
- Scaling the diode pump power using fiber-coupled diode arrays is expensive, although the most practical approach.
- Thermal management requirements are more severe for high-power end pumping, as energy deposition volumes tend to be small.

There is an additional consideration for end-pumped lasers that should be noted. Because of the high degree of alignment between the diode and the laser axis, laser light that leaks through the optical coating on the pumped face of the rod will be directed to the emitting facet of the diode. This light passes through the pump optics and could be focused onto the diode face. For moderate power cw lasers or fiber-coupled pump diodes, this is generally not a problem as the back-propagating power density at the diode face is below the damage threshold. However, for high-peak-power *Q*-switched lasers, care must be taken in the end-pumped laser design in order to avoid problems. And, if the coating on the pumped face becomes damaged, as can happen with high-peak-power *Q*-switched lasers, then the pulse energy directed toward the pump diodes will increase substantially. This can spell disaster for the diodes.

For side pumping, the advantages are

- The pump optics are inexpensive and may not even be required for laser designs that operate with the diodes "butt-coupled" to the rod.
- Power scaling is accomplished in a relatively straightforward manner by adding more arrays around the side of the gain element.
- The pumped volume in the rod is large, reducing the thermal load for a given pump power relative to end pumping.

The disadvantages are

- TEM_{00} operation is more difficult to achieve in a side-pumped geometry—there is no natural gain aperture.
- Pump efficiencies tend to be lower because a significant fraction of the pump energy is generally deposited outside the active volume.
- The dimension transverse to the resonator mode is short, which limits the absorption pathlength relative to that available for end pumping, and reduces the pump efficiency.

Returning to our laser design exercise, the specified cw output power for the laser is 1 W, so the preferred pump configuration is **end-pumped.**

3.2 Selecting the gain element

3.2.1 Laser host crystals

There is a wide variety of host crystals for trivalent Nd ions, many of which have been successfully demonstrated under diode pumping. Some have unique properties that are useful for specialized applications. For example, stoichiometric crystals allow high concentrations of trivalent Nd. Up to 100% "doping" is possible in such crystals, as the Nd ion is not interstitial but an intrinsic component of the lattice. These materials strongly absorb the pump emission, and as a consequence the gain element can be made very thin. Self-doubling host crystals produce both the fundamental and second harmonic. Such crystals generate 532-nm (green) emission directly. There are also host crystals that are more effective for producing Nd laser transitions other than the 1-μm transition. $YAlO_3$ (YALO), for example, is advantageous for generating 1.3-μm emission.

For the purpose of this section we are interested in identifying the best host for the 1-W cw laser. In general, desired crystal characteristics are

- readily available from numerous suppliers,
- growth techniques are mature, and
- manufacturers are able to routinely supply high-optical-quality, uniform Nd-doped material.

There are additional properties that are desirable for diode pumping. For one, the thermal properties must be compatible with the high-energy deposition produced by laser diodes. Diode output wavelengths match strong Nd absorption lines. Therefore, absorption depths are short, and multiwatt pump powers are typically absorbed within several tenths of a millimeter of propagation through the rod. Some of this energy is converted to heat, which can produce adverse effects such as thermally induced lensing, birefringence, and thermal fracture. Second, the absorption bandwidth of the material is important. Diode array bandwidths are several nanometers. If the Nd absorption lines are too narrow, much of the pump light will pass through the active volume, leading to low pump efficiency. For similar reasons the crystal should exhibit strong absorption at the diode wavelength. The absorption spectrum of YALO, for example, contains a series of weak absorption lines near 800 nm. Finally, the crystal should produce high optical gain.

There are three well-known host crystals that have characteristics desirable for diode pumping: YAG, YLF, and YVO_4. We will review the properties of these crystals briefly, highlighting the crystal criteria noted above. Crystal properties are summarized in Table 3.2.

Table 3.2. Host crystal properties.

PARAMETER	**YAG**	**YLF**	**YVO_4**
crystal structure	isotropic	uniaxial	uniaxial
σ_{em} (10^{-19} cm^2)	6	3	30
τ_f (μs, 1% doping)	230	480	100
Thermal conductivity (W/cm K)	0.13	0.06	0.05
dn/*dt* (10^{-6} K^{-1})	7.3	−4.3(e) −2.0(o)	8.5
Peak absorption wavelength (nm)	808.5	792	810
Absorption coefficient at peak (cm^{-1}, 1% doping)	8*	32	41
Absorption bandwidth (FWHM, nm)	1	3	8
Knoop hardness (kg/cm^2)	1320	260	480
laser wavelength (nm)	1064.2	1.047 (e) 1.053 (o)	1.0641 (e) 1.0664 (o)
linewidth (nm)	0.6	1.2	0.8
refractive index at laser wavelength	1.818	1.4704 (e) 1.4481 (o)	2.168 (e) 1.958 (o)

YAG

YAG, or yttrium aluminum garnet ($Y_3Al_5O_{12}$), is the most commonly used material for Nd-doped lasers. Although many commercial diode-pumped lasers are now being produced with YVO_4 hosts, YAG possesses numerous features important for diode pumping. It has a large Knoop hardness (important to prevent breakage during fabrication), high gain, and high thermal conductivity. Nd doping concentrations are limited to about 1% due to the diameter of the Nd ion relative to the Y ion (for which Nd is substituted). This concentration is sufficient to produce efficient laser operation. YAG is isotropic, and therefore the laser output is not polarized. In addition, the absorption cross section is not polarization-dependent, which is an important consideration when pumping with crossed or random polarization.

YLF

YLF, or $LiYF_4$, is a uniaxial crystal that produces linearly polarized laser emission. One important application for YLF is high-power excitation where polarization-sensitive losses are present in the cavity. The natural birefringence of YLF overwhelms the thermally induced birefringence. As a consequence, polarization losses do not increase with increasing output power. The gain and thermal conductivity for YLF are lower than YAG, but the lifetime is more than a factor of two longer. This last factor is important for *Q*-switched operation. Referring to the discussion above that compares side and end pumping, it was noted that a 1-J/pulse Nd:YAG laser requires 19 kW of diode pump power. This was calculated using a 150-μs pulse. For YLF, one can use pulses as long as 500 μs, and, assuming the same efficiency factors, the pump diode power required to produce a 1 J pulse in YLF is reduced to 6 kW.

Unfortunately, thermal fracture is a greater problem in YLF than YAG, and the resonator design must provide efficient cooling, particularly for high-power operation.

YVO_4

Yttrium orthovanadate, YVO_4, is often referred to as “vanadate.” Vanadate is a uniaxial crystal that produces a linearly polarized output. This crystal has become the favorite of many commercial diode-pumped laser suppliers because it combines the desirable properties of a large absorption bandwidth and high gain. A wide absorption bandwidth is desirable from the viewpoint of matching the broad emission bandwidth of the pump diodes. The short fluorescence lifetime is an advantage for high-repetition-rate *Q*-switched laser operation. As noted in the discussion on YLF, the short lifetime means low energy storage, which is not a desirable property for applications requiring high energy/pulse. However, for cw or high-repetition-rate *Q*-switched operation, the short vanadate lifetime is not problematic.

A significant disadvantage of vanadate for diode pumping is the large thermal lens produced even at moderate pump powers. Thermal lensing must be compensated in vanadate lasers, and this prevents its use in certain resonator configurations.

The specifications of our working example call for an unpolarized output beam, so we will select **Nd:YAG** as the laser gain element.

3.2.2 Laser rod specifications

The peak absorption coefficient for Nd:YAG is approximately 8 cm^{-1}. This means that the absorption length (or 1/*e* attenuation depth) for 808.5-nm pump light is 1.25 mm. Beer’s law absorption is multiplicative in absorption depth, so that 63% of the pump light is absorbed in the first 1.25 mm, 86% is absorbed by the time the beam has traversed two absorption lengths, 95% in three, and 98% in four. The fraction of light absorbed (A) in the crystal is

$$A = 1 - e^{-\alpha\ell}\ , \tag{3.1}$$

where α is the absorption coefficient and ℓ is the pathlength in the crystal. A 5-mm pathlength in the rod will result in 98% absorption of the incident light at 808.5 nm. In general, the rod length and doping density should be adjusted so that the $\alpha\ell$ product is at least 2 for diode pump light at the FWHM wavelength points. The absorption coefficient at wavelengths corresponding to the FWHM points is 4 cm^{-1}. As the FWHM of the Nd:YAG absorption line is comparable to the spectral bandwidth of the pump diode, more than 90% of the entire pump beam will be absorbed if the crystal pathlength is 10 mm. Since there is little penalty for making the rod longer than necessary, **we will select a 1-cm-long Nd:YAG crystal. The doping density is 1.1%**, which is standard for Nd:YAG and is required in order to achieve the 8 cm^{-1} absorption coefficient. Finally, **the rod diameter is selected to be 6.4 mm** (.25 inch). The diameter can be substantially smaller: 2 or 3 mm is often used. However, the 6.4-mm diameter allows for a more rigid rod, which is less subject to fracture and can be easily accommodated in macroscopic optical mounts.

3.3. Selecting the laser diode

3.3.1 Pump diode center wavelength and spectral bandwidth

Having selected the laser gain element, the center wavelength and bandwidth are determined by the specifications listed in Table 3.2 for Nd:YAG. These are **808.5 nm** and **1 nm**, respectively. Two 1-W cw single-stripe diodes are required to produce the 1-W Nd:YAG laser output power as specified in Table 3.1. The following sections describe the spectral characteristics of these diodes.

3.3.2 Temperature tuning

The center wavelength of a laser diode shifts with junction temperature by +0.3 nm per centigrade degree. Individual diodes can be wavelength selected when ordered from the manufacturer, but usually the selection is within a ±3-nm window. That is, if an 808-nm diode is ordered, the vendor will ship a diode ranging between 805 nm and 811 nm. Diode lifetimes decrease dramatically as the operating temperature increases, and it is therefore better to use a diode that produces a wavelength that is somewhat too high rather than too low. For example, a diode rated to produce 1 W of 810-nm emission at 25°C will require cooling to bring the junction temperature down to approximately 19°C in order to produce output at 808 nm. On the other hand, an 806-nm diode would require an operating temperature of approximately 31°C to produce 808-nm emission.

There are some practical issues to note regarding diode cooling. First, the thermal conductivity of the semiconductor substrate is quite low, so a significant amount of cooling is required just to keep the junction at 25°C. That is, the chip substrate will generally have to be maintained at 15 to 20°C in order for the junction to remain at 25°C. This 5 to 10°C temperature differential is constant over the range of temperatures used for diode pumping, so the 19°C junction temperature required for an 810-nm diode to produce 808-nm output would require cooling the chip in the range of 9 to 14°C. This is not difficult to do. However, care must be taken to consider the dew point of the operating environment. Water condensation on the diode or on the optical window of a hermetically sealed housing will degrade the laser diode output. An additional caution is that cooling should be applied only when running the diode, as the diode may otherwise get too cold when the drive current is not heating the junction.

An interesting aside involving diode cooling is that the optical output at constant current increases for these diodes at the rate of 3.8 mW/°C. The variation in diode output spectral properties with heat sink temperature is shown in Fig. 3.2. A 1-W Sony laser diode in a 9-mm housing was used for this measurement. The diode case temperature is indicated for each spectral trace.

3.3.3 Bandwidth control

There is little that an end-user can do to change the laser diode output bandwidth. For diode arrays the output bandwidth is generally ±2 nm, although arrays with narrower bandwidths can sometimes be specified. The 1-W broad-stripe laser diodes selected to pump the Nd:YAG laser typically emit eight longitudinal modes simultaneously, each separated by 0.3 nm. These modes are readily visible in the spectral traces shown in Fig. 3.2. The FWHM bandwidth is about 1.2 nm, a good match to the Nd:YAG rod absorption bandwidth. Alternatives for obtaining pump diodes with narrower output bandwidths include single-mode diodes, commercially available in power levels up to 200 mW; single-mode MOPA configurations, commercially available in power levels up to 1 W (but very expensive); and do-it-yourself injection-locked laser diodes or homemade MOPAs.

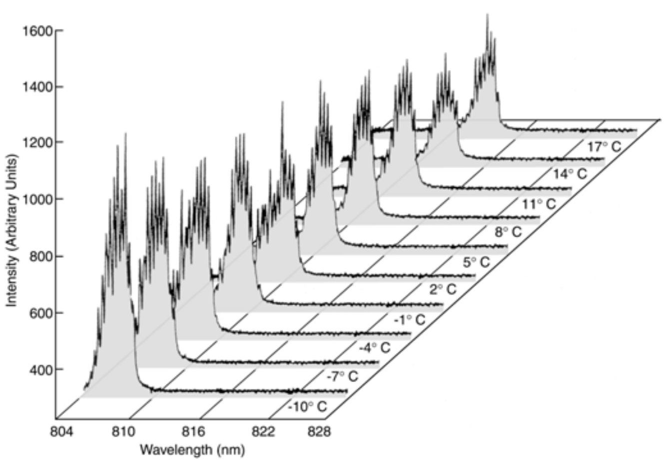

Figure 3.2. Temperature dependence of the output spectrum of a 1-W laser diode.

3.3.4 Current tuning and mode hop

As the diode output power is increased by applying more current to the junction, the temperature increases, thereby red-shifting the diode output wavelength. For qcw diodes, the temporal injection of current into the junction produces a variable emission spectrum and hence pump efficiency. A second effect related to the drive current is tuning due to the changing density of electrons in the junction. The electron density affects the refractive index of the active layer and determines the frequencies of the Fabry-Pérot resonator modes. The wavelength shift due to current density changes is about 0.03 nm/A.

Mode hopping is a phenomenon that prevents continuous tuning of a laser diode output wavelength over a range that is wide compared to the intermodal spacing. As mentioned above, diode resonator modes are separated by 0.3 nm. These modes are superimposed on the broad spectral gain profile of the active layer. As the temperature changes, the peak of the gain spectrum shifts. At some point, the gain for the wavelength represented by an adjacent longitudinal mode will be higher than the gain at the longitudinal mode that has been oscillating. At this point, the diode demonstrates an instability or "mode hop." The output wavelength shifts discontinuously from the n^{th} mode to the $(n\pm1)^{\mathrm{th}}$ mode.

3.4 Selecting the resonator

3.4.1 Resonator length

The overall resonator length is not critical for the Nd:YAG laser. However, there are several factors that recommend a short resonator. For one, the longer the length, the more cumbersome the alignment. In addition, "miniaturization" is a strong commercial influence that dictates a short resonator. Finally, long resonators that are nearly hemispherical are less stable due to increased sensitivity to vibration or factors that cause slight changes to the resonator optical length such as temperature or air currents.

It is interesting to note, and perhaps not immediately obvious, that the resonator configuration and not the resonator length determines the mode waist size. It is possible, although not necessarily practical, to achieve a relatively small waist in an arbitrarily long resonator. Referring to Eq. (2.1), for example, we see that the dependence of the nearly hemispherical resonator waist on the resonator length is dependent on the factor g_2. So for any given radius of curvature mirror, long or short, the value of L/R_2 can be set close enough to 1 to produce a small waist. In fact, we know that the waist diameter will vanish when $L=R_2$, independent of the value of L. However, precise mirror location and the overall resonator stability become important issues for long resonators. Achieving a very small waist with a large L allows little tolerance for mirror motion.

A graphical way to see that the overall resonator length does not in itself determine the mode waist size is to first note that the mode wavefront in Fig. 2.1 is curved. The wavefront radius increases as the wavefront moves from the flat mirror to the curved. Indeed, at mirror 2 the wavefront curvature matches the radius of curvature of the mirror. We can now imagine another mirror with a larger radius of curvature. If we place this mirror further away from the flat, at a location where its radius of curvature matches the ever-expanding radius of the resonator wavefront, we will have a stable, nearly hemispherical resonator mode identical to that shown in Fig. 2.1. Although the overall resonator length will be greater, the mode waist is identical. Of course, the reader may note that the spot size on mirror 2 will be larger under these conditions, increasing the diffraction loss. Therefore, we should increase the mirror diameter to constrain these losses.

There are other issues to consider in designing the resonator length. What is the availability of high-quality short-focal-length resonator optics, and what are the manufacturing tolerances? For example, mirrors with radii of curvature shorter than 5 cm are difficult to manufacture. Also, the resonator should be long enough so that the intracavity components can be readily accessed for cleaning, alignment, etc.

Additional length considerations are relevant when certain intracavity components are used in the resonator. For *Q*-switched operation, the pulse width increases with the cavity length, so to enhance the peak output power it is desirable to have a compact resonator. The *Q*-switched pulse length is a multiple of the cavity decay time τ_c, which is defined as the time for light in the resonator to decay to $1/e$ of its original intensity. The decay time is given by

$$\tau_c = \frac{2Ln_i}{c\xi} \quad , \tag{3.2}$$

where ξ are the resonator losses including the output mirror transmission T, and c is the speed of light. As the resonator length L increases, τ_c increases, and therefore the *Q*-switched pulse length increases as well (assuming all other factors remain constant). For a fixed τ_c, the pulse width decreases as the ratio of the (pump-power-dependent) gain to the passive loss increases.

On the other hand, for intracavity SHG, beating between two simultaneously oscillating longitudinal modes produces instability in the second harmonic emission intensity. As discussed above, the frequency separation between adjacent modes varies inversely as the cavity length. Longer cavities can support a greater number of longitudinal modes and therefore produce more stable second harmonic output power.

Based on the common availability of 10-cm radius of curvature (ROC) mirrors and the previously selected Nd:YAG rod length of 1 cm, the **overall cavity length is set to 10 cm**.

3.4.2 Resonator configuration

The most important consideration for determining the resonator configuration is the pump power density. The rod is to be pumped with about 2 W of diode power. Threshold pump power densities for Nd:YAG are several kilowatts per square centimeter, while thermal loadings in excess of hundreds of kilowatts per square centimeter can be sustained before adverse effects on the laser performance are observed. As will be seen in Chapter 4, both the threshold pump power and the slope efficiency depend inversely on the resonator mode waist. Keeping the resonator mode waist small suggests either a hemispherical or confocal resonator design. A mode waist of approximately 75 μm will produce the appropriate pump power density.

Confocal resonators are not generally efficient for low to moderate output power, as the mode waist tends to be too large for pump power levels of several watts. Another difficulty with the confocal resonator is that the beam waist is located between two concave end mirrors, requiring the pump diode focusing lens focal length to be longer than it would be were the waist located at the end mirror. This will produce a larger pump spot size and lower pump power density, raising the threshold and lowering the slope efficiency. In addition, if the pump spot is larger than the resonator mode waist, energy is deposited outside the boundaries of the TEM_{00} mode, and consequently the pump efficiency will be lower.

These observations lead to the conclusion that the **resonator configuration should be nearly hemispherical,** with the separation between the flat and curved mirror adjusted to produce an approximately 75-μm waist at the flat mirror. Furthermore, the exterior face of the rod is HR coated to act as the flat mirror. This not only replaces one of the optical components but also allows the resonator waist to be located at the pumped end of the laser rod. Thus, by focusing the diode pump emission on the exterior face of the rod, the pump and resonator mode waists coincide to produce highly efficient end-pumped laser operation.

3.4.3 Rod coatings

The exterior face of the Nd:YAG rod has a dichroic coating that is HR at 1.06 μm and highly transmissive (HT) at 808 nm to allow maximum transmission of the pump light. The interior face is AR coated for 1.06 μm. The concave mirror is coated for 97% reflectivity at 1.06 μm. This provides the highest output power. The optimum mirror reflectivity will be discussed in the next section.

The end-pumped laser is beginning to take shape, and is illustrated in Fig. 3.3.

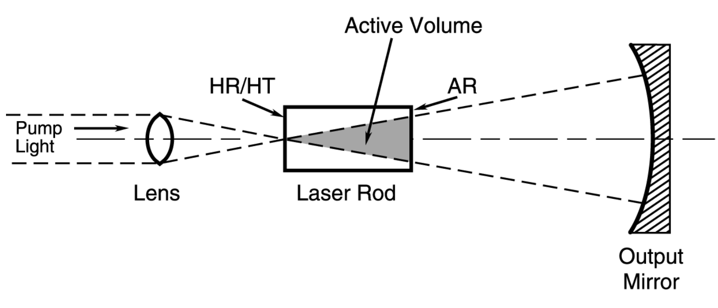

Figure 3.3. Schematic of the end-pumped nearly hemispherical laser resonator.

3.5. Selecting the pump optics

3.5.1 Pump optics

Selection of the pump optics represents the most critical choice for efficient end-pumped laser operation. The issues for the pump optics revolve around the unique output characteristics of laser diodes, particularly their high output divergence. Pump optics include collimating lenses as well as a focusing lens for generating a pump waist on the exterior face of the laser rod. (Actually, the best location for the pump waist is near the exterior face, inside the rod. This will be discussed in detail in Section 3.5.3.)

3.5.1.1 NA

As discussed previously, the lens NA is related to the solid angle of light that is collected by the optics. For the laser diode to effectively pump the gain medium, the light must first be collimated. The collimated beam can then be focused onto the laser rod. For the collimating lens, the minimum NA is determined by the divergence of the laser diode emission in the plane perpendicular to the junction. Divergence in this plane ranges from about 25° to 40° FWHM, depending on the vertical confinement of the diode light within the active layer. The 1-W Sony laser diode used in this design (SLD 304V) is rated to produce a 28° divergence FWHM in the perpendicular plane.

The appropriate NA for the lens can be determined using the definition of NA presented in Eq. (2.8). We want to use a lens that will collect and collimate as much of the diode light as possible, but based on the large angle involved, a reasonable design point centers on a solid angle that is at least twice the divergence angle. Using α_m=28° and an n_0 of 1, the minimum NA is 0.47 (note that the FWHM angle is twice the solid angle, and the solid angle for this diode is 14°). With this NA, about 80% of the light is collected.

Since the divergence in the plane parallel to the junction is only 9° FWHM, a high- NA lens will collect all of this light. However, light emitted in the plane parallel to the junction will not be collimated by the spherical lens, a point that will be discussed further in relation to astigmatism.

3.5.1.2 Working distance

In general, the working distance of lenses used for diode pumping should be as short as practical. The working distance for the collimating lens represents the distance between the object side of the lens housing and the object itself. The Sony laser diode is packaged in a 9-mm can to protect the diode from the environment. The distance between the diode-emitting facet (approximately the "object") and the front edge of the can is 1.1 mm. The glass window on the can is recessed with respect to the edge and is 230 μm thick. A compound lens with an NA of 0.5 and a working distance of 1.13 mm is commercially available and suitable for collimation. This lens can be purchased with an integral compensator for window-induced spherical aberration, but this is important only for window thicknesses that exceed 300 μm. The NA of 0.5 allows collection of light within a solid angle of 30° (60° FWHM), which in the case of the Sony diode amounts to a collection efficiency of approximately 90%.

3.5.1.3 AR coating

Antireflection (AR) coatings on the collimating and focusing optics are important both for high transmission as well as preventing feedback into the laser diode. High-NA compound lenses often have multiple optical surfaces. The specific lens used for collimation in this exercise has three elements or six surfaces. If the lenses were completely uncoated, the light throughput would be only about 75%.

Feedback is a major concern as well. Feedback due to reflected light re-entering the active layer of the laser diode causes both amplitude and wavelength instabilities. Although the lens surfaces are curved, the working distances are short enough so that a substantial fraction of the reflected light will re-enter the active layer. Instability is only one problem caused by feedback. A potentially more serious problem is facet damage. The optical flux passing through the diode facet is near the threshold for optical damage. If a significant amount of output light is reflected back into the active layer, a second, "parasitic" resonator is established between the collimating lens and the emitting facet. This can substantially increase the flux incident on the facet and enhance the possibility for permanently damaging the laser diode.

The properties of the collimating lens selected for the 1-W cw laser diode are summarized as follows:

focal length	8.0 mm
clear aperture	8.0 mm
NA	0.5
working distance	1.13 mm
minimum spot size	1.02 μm at 830 nm
wavefront distortion	$< \lambda/4$
coating	AR single layer, < 1% reflectivity overall

Certainly it is possible to improve upon the selected pump optics. Lenses with higher numerical apertures are available to collect more of the pump light, as are lenses with high-quality multilayer dielectric AR coatings to transmit more of the collected pump light. However, the lens listed above is relatively inexpensive and is useful for demonstrating the diode-pumped laser.

3.5.2 Astigmatism correction

Laser diode output beams are astigmatic so that the spherical lens used to collimate light emitted along the "fast axis" (light in the plane perpendicular to the junction) will converge with light emitted along the “slow axis.” This is because the light emitted in the plane parallel to the junction is almost collimated, diverging at only 9° FWHM. Another way to view diode astigmatism is to envision two axially separate point sources, one for each of the two emission planes (parallel and perpendicular to, respectively, the plane of the junction). To correct for astigmatism, which typically amounts to 70–100 μm of axial separation of the two point sources, an anamorphic lens system is required. Such a system is shown in Fig. 3.4. In this arrangement, collimation is provided by a pair of lenses, one spherical and one cylindrical. In the fast axis, collimation is produced by the spherical lens (S.L. 1). The cylindrical lens (C.L. 1) is oriented with zero power in the perpendicular plane. In the slow axis collimation requires the pair of lenses. S.L. 1 focuses the emerging light, while C.L. 1 recollimates it. Therefore, the light incident on the focusing lens (S.L. 2) is collimated. The cylindrical lens used is an AR-coated high-optical-quality 100-mm focal length lens.

3.5.3 Focusing lens

Up to this point we have been concerned with the collimating optics. As illustrated in Fig. 3.4 the anamorphic lens pair collimates the emission from the laser diode, which in turn is focused with a spherical lens. A short-focal-length spherical lens is desired to produce a small spot size in the focal plane. The exterior face of the rod also serves as the end mirror for the resonator so that very short working distance optics can be used. An important issue in the selection of the focusing lens is the magnification, which is the ratio of the focal length of the focusing lens to that of the collimating spherical lens. Since the fast axis is diffraction limited and the image dimension in the perpendicular plane is only a few microns, the limiting factor for pump power density is the horizontal dimension of the pump spot.

The optical system shown in Fig. 3.4 produces an image in the focal plane of the laser diode far-field. Furthermore, the dimension of the image in the parallel plane is reduced relative to the emitting aperture or stripe width of the diode. The reason for this is that although the divergence is many times diffraction limited, the output is partially coherent. When focused, the spot in the parallel plane is therefore smaller

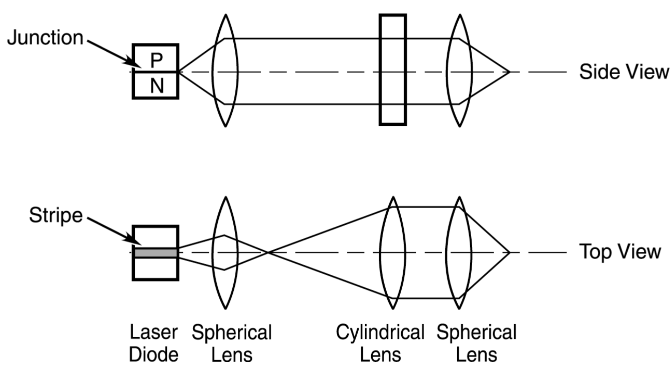

Figure 3.4. Anamorphic optical system[1] for diode pumping.

than the emitting aperture. Using a focusing lens identical to the collimating lens provides excellent pump power density in the rod. The diode far-field pattern is shown in Fig. 3.5, and the intensity pattern in the focal plane is shown in Fig. 3.6. Note the structural similarity between the intensity patterns in the two figures. Fig. 3.6 indicates that extent of the horizontal dimension of the image in the focal plane is 75 μm, with the two lobes separated by approximately 50 μm. Thus, the pump spot diameter is approximately twice the resonator mode diameter. This is desirable, as will be shown in this section as well as in Sections 4.1 and 4.5.3.

Another important criterion for selecting the focusing lens is the divergence or NA. The ideal pump optical system would generate a small focused spot with a narrow beam divergence. The low divergence is desirable to assure that the pump light does not expand outside of the boundary established by the active volume in the rod. Unfortunately this is not possible, because the smaller the pump spot, the higher the beam divergence. An approach to producing an efficient pump beam within these constraints is shown in Fig. 3.7. The pump light is focused inside the rod instead of at the exterior face. The resonator mode size is adjusted so that the resonator waist matches the input pump beam radius at this face. The pump light continues to converge as it propagates toward the focal plane while the resonator mode expands. Beyond the focus the pump beam diverges, and eventually expands outside the boundary of the active volume. However, the point at which the pump flux passes outside the active volume occurs at approximately 5 mm into the rod. Because of absorption there is little or no intensity left in the pump beam at this point, the majority of the pump energy having been deposited within the active volume.

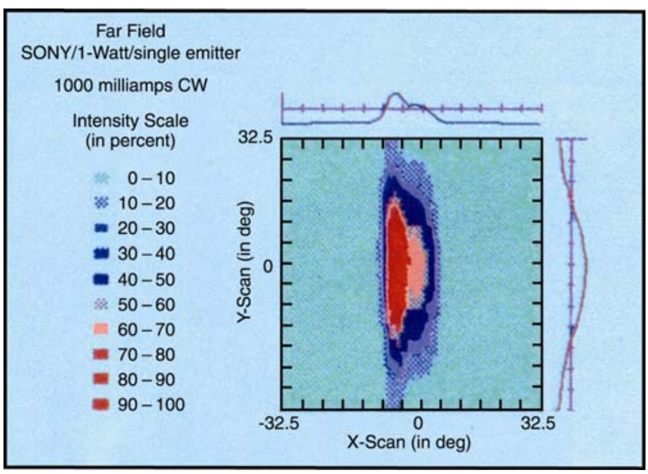

Figure 3.5. Measured far-field pattern of the 1-W Sony laser diode. Lines above and to the right of the far-field pattern show intensity traces through the center of the emission pattern in the parallel and perpendicular planes, respectively. Each tick mark represents 5º, and the crossing of the intensity trace with the axis represents the half-intensity point. The orientation of the junction is parallel to the x-axis. Notice the two lobes in the intensity trace in the parallel plane.

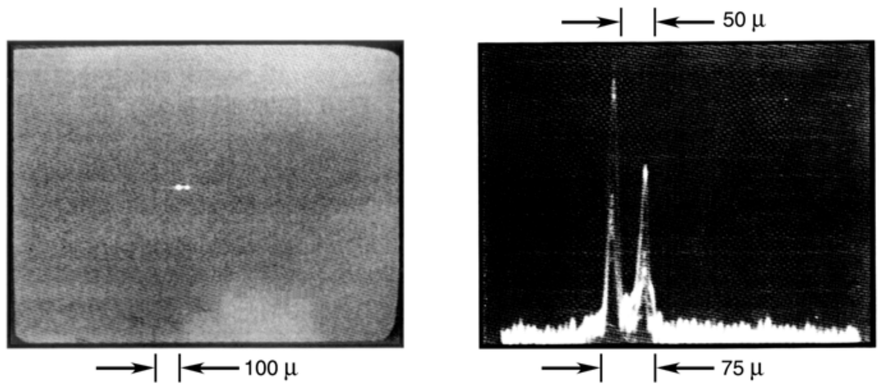

Figure 3.6. Intensity patterns of the 1-W Sony laser diode in the focal plane. The image on the left is the actual twin-lobe pattern produced by the pump optics in the focal plane. The image was taken with a 7X magnifcation using an infrared-sensitive video camera. The image on the right is an oscilloscope trace of the video lines containing the twin-lobe image shown on the left.

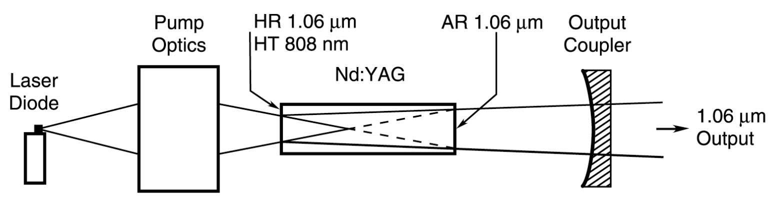

Figure 3.7. End-pumped geometry.[2]

Note that for a stable resonator the spatial distribution of energy deposition within the TEM_{00} active volume does not affect the output intensity distribution. Unless thermal gradients or other inhomogeneities are established by the pump beam, the circulating fluence integrates across the gain distribution in extracting energy. That being said, an additional benefit of this pumping technique is that thermal loading will be reduced while maintaining high pump efficiency. This is true since the pump power density is lower than when focusing directly on the rod face. At full power the pump beam enters the rod with a larger diameter than it would have if it were focused at the face, while at the focus the power density is diminished by prior absorption in the rod.

3.5.4 Polarization combination of laser diodes

Two 1-W laser diodes are required to produce the desired Nd:YAG output power. Because of the high degree of overlap required between the pump beam and the resonator mode, angular multiplexing is generally inefficient. Several techniques for end pumping with multiple laser diodes will be presented in Part III, but polarization beam combination, perhaps the most well known technique, is discussed in this section.

Polarization beam combination, one of the first techniques used to increase the laser diode pump power for an end-pumped laser, is illustrated in Fig. 3.8. The diode output is strongly polarized in the parallel plane. Commercially available polarization beam splitter cubes have been available for many years. These cubes are efficient beam separators for linearly polarized light, transmitting one polarization and reflecting the orthogonal one. By using the polarization beam separator in reverse it becomes a polarization beam combiner (PBC). As shown in Fig. 3.8, two diodes are oriented in relation to the PBC so that the output polarization of each is orthogonal. As a consequence, the emission from one diode is reflected, while the other is transmitted. This produces a single pump beam containing the output power from both diodes. The combined beam includes both polarizations, and therefore this technique may not be appropriate for crystals that have strong polarization-sensitive absorption coefficients. However, Nd:YAG is isotropic and polarization combination is highly effective for scaling the pump output power.

High-quality PBC cubes are available from several manufactures, and the device operation is illustrated in Fig. 3.9. Cubes specifically designed for operation with AlGaAs laser diodes are manufactured with AR coatings on the entrance and exit faces. The surface reflectivity is generally less than 0.25% per surface. Typical specifications for a commercial PBC are 98% transmission for the *p* polarization; 99% reflection for the *s* polarization; surface figures are $\lambda/10$; and peak-to-peak wavefront distortion is $\lambda/4$.

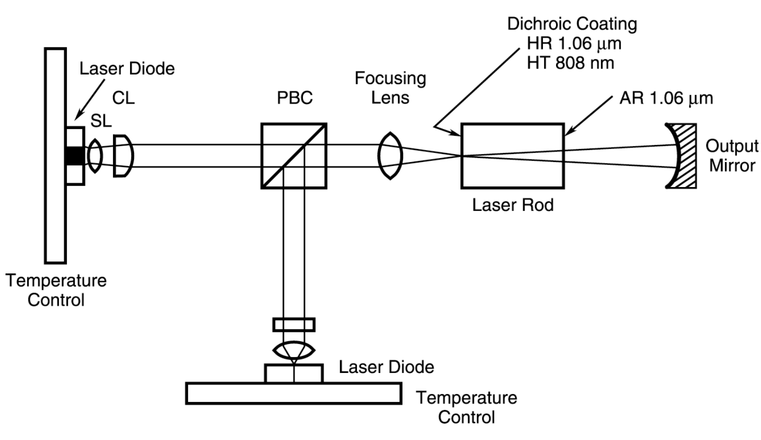

Figure 3.8. End pumping using polarization beam combination.

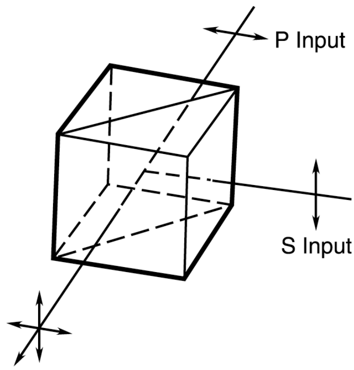

Figure 3.9. Operation of a polarization beam combiner.

Referring to Fig. 3.9, it can be seen that a collimated beam is required for efficient PBC operation. This requirement eliminates the possibility of utilizing true relay optics in the end-pumping geometry. That is, astigmatism issues aside, one might ask why a single spherical lens could not be used to relay the image of the diode output facet onto the Nd:YAG laser rod. It can, of course, and many laser designs use a single lens for the pump optics. However, there are certain limitations that accompany the simplicity of the single-lens pump optics. For example, this approach inhibits the use of polarization beam combination as a means for increasing the diode pump power. In addition, and more importantly, the diode output facet is 200 μm wide (the stripe width). Even with a reasonable amount of demagnification, the facet image at the rod will be larger than the 75-μm-wide spot illustrated in Fig. 3.6. The diode facet image produced by a true relay lens system is that of the diode near-field, while the image produced by the optical system illustrated in Fig. 3.4 is that of the diode far-field.

3.5.5 Diffraction-limited operation

One final note before concluding this section: the term "diffraction-limited" has been used in the text but not defined. Diffraction-limited operation represents the best performance level for an optical system. Diffraction-limited divergence is given by

$$\theta = \lambda/\pi w_0 , \tag{3.3}$$

where θ is the half-angle divergence and w_0 is the beam waist. The diffraction-limited spot size w_s, obtained when a diffraction-limited Gaussian beam is focused, is given by

$$w_s = f\theta , \tag{3.4}$$

where f is the focal length of the lens.

Chapter 4

Operation of the Continuous-Wave Diode-pumped Laser

In this chapter we discuss the performance of the laser designed in Chapter 3 and compare it with theoretical predictions. The efficiency factors are examined in detail to provide a fundamental appreciation of their effect on the overall device performance.

4.1 Resonator gain and loss: Findlay-Clay analysis

The passive resonator loss is an important determinant of laser performance. Losses due to scattering, absorption, and leakage through HR coatings increase the laser threshold power while decreasing the output power for a given pump power. There are two methods commonly used to measure the resonator passive loss. The first measurement technique uses the relaxation frequency of the damped emission oscillations resulting from an optical excitation pulse. This measurement is well documented in the literature,[3] and the resonator passive loss L_p (including output coupling) can be obtained from

$$L_p = (2\pi f_r)^2 \frac{2\tau_f (n_1\ell_1 + n_2\ell_2)}{P_e c}, \qquad (4.1)$$

where f_r is the relaxation frequency, P_e is the excess energy given by

$$P_e = (P - P_{th}) / P_{th}, \qquad (4.2)$$

P is the absorbed pump power, P_{th} is the threshold pump power, and $n_i\ell_i$ represent the refractive index and pathlength, respectively, of the Nd:YAG rod and air. This technique provides the value of the passive resonator loss in a single measurement.

The Findlay-Clay analysis represents a more involved series of measurements. In this technique the threshold power is determined as a function of the output coupler mirror reflectivity R. The data points are plotted as $-\ell n\, R$ *vs* P_{th} and are fit to a straight line by linear regression. The slope of the line is proportional to the small signal gain g_o and is given by

$$\text{slope} = 2g_o\ell / P\,, \tag{4.3}$$

where ℓ is the rod length. The value at the intercept of the linear regression line fit with the $-\ell n\, R$ axis is equal to the round trip loss. The advantage of this technique is that it not only produces a value for the resonator loss but also for the small signal gain.

The Findlay-Clay data for the laser designed in Chapter 3 is shown in Fig. 4.1. The linear regression fit to the data provides a slope of 8.1×10^{-4} mW^{-1} and a round trip loss of 0.0009 or 0.09%. The small signal gain is an important laser parameter that determines the amplification of the gain medium. The small signal gain for a laser is given by

$$g_o\ell = \frac{\eta_p P}{I_{sat}(A_p + A_m)}\,, \tag{4.4}$$

where A_p and A_m are the area of the pump and resonator modes, respectively, and η_p is the pump efficiency. The pump efficiency is the fraction of the absorbed pump light converted to laser output and is often called the optical conversion efficiency. I_{sat} is the saturation fluence and is an important material parameter given by

$$I_{sat} = h\nu/\sigma_{em}\tau_f\,. \tag{4.5}$$

For the 1.06-µm transition in Nd:YAG, $h\nu$ is 1.9×10^{-19} J, τ_f and σ_{em} are listed in Table 3.2, and I_{sat} is 1.35 kW/cm^2. Comparing the expression for gain with the

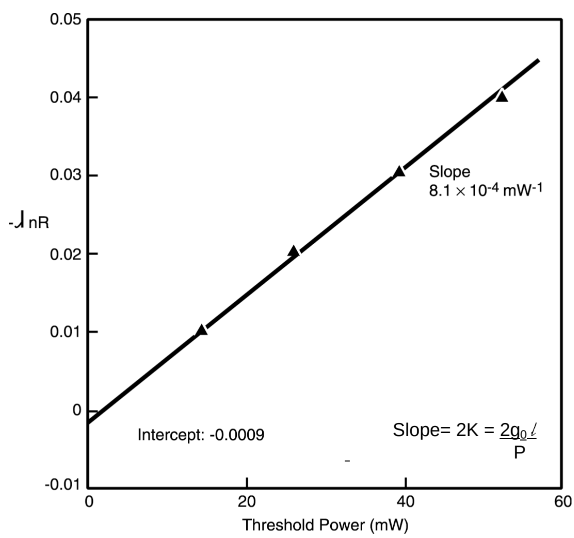

Figure 4.1. Findlay-Clay data for the Nd:YAG end-pumped laser.

equation for the slope of the linear fit to the Findlay-Clay data,

$$\text{slope}/2 = \eta_p\ /[I_{sat}(A_p + A_m)]. \tag{4.6}$$

The value for A_p is the average area of the pump beam in the crystal. This number depends on the focusing lens NA, the emission bandwidth of the laser diodes, and the absorption coefficient of the laser rod. The focused spot size in the crystal is roughly 5 μm by 75 μm or 3.75×10^{-6} cm^2. The beam divergence in the crystal due to the NA 0.5 lens produces an average pump beam diameter A_p over several absorption lengths of approximately 2×10^{-5} cm^2. On the other hand, the laser resonator mode area is significantly larger as the waist cross-section is circular and must be large enough to circumscribe the horizontal dimension of the pump mode as it enters the rod. The resonator mode diameter at the pumped face of the rod should be approximately two times the horizontal dimension of the spot in the focal plane. Over the first several absorption lengths in the crystal, the beam diameter expands somewhat, but we can obtain a good estimate of the average resonator mode size from the expression[4]

$$A_m = \frac{2P_{th}\tau_f\sigma'}{L_p h\nu}, \tag{4.7}$$

where σ' is the effective cross section (3.2×10^{-19} cm^2 for Nd:YAG) and, as noted above, L_p is the sum of the round-trip resonator loss (L_r) and the output coupling. From the known values of the parameters in the above expression, $A_m = 9.5\times10^{-4}$ cm^2 and the average resonator mode radius in the crystal is 175 μm. Using these values in the equation for the slope, and assuming η_p is 0.5, we get

$$\text{slope}/2 = 0.5/[1350\ (2\times10^{-5} + 9.5\times10^{-4})]\ =\ 3.8\times10^{-1}\ \text{W}^{-1}.$$

Converting the Findlay-Clay slope to mW^{-1} from W^{-1} we find good agreement between the experimental (8.1×10^{-4} mW^{-1}) and the calculated (7.6×10^{-4} mW^{-1}) slope. The importance of introducing Eq. (4.4) for calculating the gain is to underscore the inverse dependence of the gain on the pump and resonator mode sizes.

4.2 Threshold

As a result of the dependence of the threshold power on the gain, the threshold varies directly with the pump and beam areas. The larger the area, the larger the threshold pump power. The pump threshold power can be written as

$$P_{th} = \frac{h\nu_p(A_p + A_m)}{4\sigma_{em} f_2\tau_f\ [1-\exp(-\alpha\ell)]}(L_r - R + 1), \tag{4.8}$$

where f_2 is the fraction of the total $^4F_{3/2}$ population in the R_2 upper laser Stark level (about 0.40 at room temperature), ν_p is the optical frequency of the pump photon, and α is the absorption coefficient of the laser rod at the diode output wavelength. With $h\nu_p = 2.45\times10^{-19}$ J, σ_{em}, f_2, A_m, A_p, and τ_f given previously, $1-e^{-\alpha\ell} = 0.98$ and $L_r = 0.0009$, we obtain

$$P_{th} = 1100\,(1.0009-R)\text{ mW}. \tag{4.9}$$

With $R = 0.97$ we obtain $P_{th} = 34$ mW, which is in good agreement with the measured value of 38 mW.

4.3 Optimum output coupling

The best output was obtained with a 97% reflective output coupler. The optimum output coupling can be calculated if the resonator gain and loss are known using the expression

$$T_{opt} = 2\left(\sqrt{0.5 g_o \ell L_r} - 0.5 L_r\right). \tag{4.10}$$

The ability to calculate T_{opt} from the measured gain and loss parameters is in fact a compelling reason to perform the Findlay-Clay resonator analysis. For an absorbed pump power of 1.6 W, the single pass gain is $1.6 \times 8.1\times10^{-1} \times 0.5 = 6.5\times10^{-1}$. The single pass loss ($L_r$ / 2) is 0.00045, giving a T_{opt} of 3.3×10^{-2}. This agrees well with the empirically determined value of 97% for the optimum mirror reflectivity.

4.4 Laser output, slope efficiency and bandwidth

4.4.1 Output

The output power for the diode-pumped Nd:YAG laser is shown in Fig. 4.2. The slope efficiency for the 97% reflective output mirror is 0.58 and the maximum output power obtained is 874 mW. This output power was produced with an absorbed pump power somewhat less than 1.6 W. The quantum defect limited slope efficiency, which is determined by the ratio of laser photon energy to pump photon energy, is 0.76. This is the maximum output slope efficiency that can be achieved, and the slope efficiency of 0.58 represents 76% of the maximum.

The output power is somewhat lower than the 1 W specified in Table 3.1. Presumably, 225 mW of additional pump power would have to be deposited in the active volume to produce the full 1-W output power.

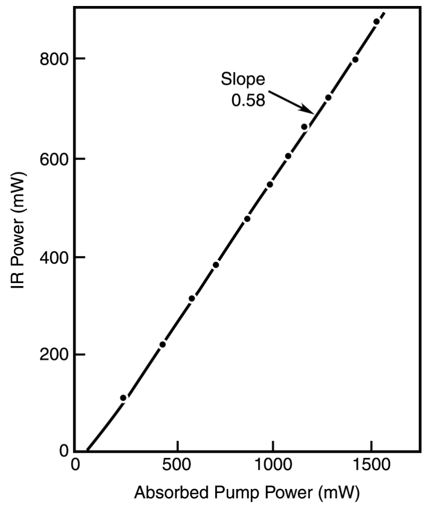

Figure 4.2. Laser output power as a function of absorbed pump power.

4.4.2 Slope efficiency

Analytical models of the slope efficiency for end-pumped lasers have been published,[5,6] and these show that the slope efficiency is highest when the ratio ("*a*") of the pump waist to the resonator waist is less than one. Since increasing the resonator waist to bring the ratio down increases the threshold pump power and reduces the gain, an efficient laser will have both small pump and resonator waists and an "*a*" value of 0.5 or less. This rule applies only to lasers that exhibit low reabsorption loss relative to the fixed resonator loss.[6]

4.4.3 Bandwidth

The laser produced TEM_{00} emission. The output spectrum was displayed on an optical spectrum analyzer and showed eight longitudinal modes operating simultaneously. The cavity mode separation can be calculated from

$$\Delta\lambda = \lambda^2 / [2\Sigma_i n_i \ell_i] = 0.0057 \text{ nm.} \tag{4.11}$$

The frequency separation is 1.5 GHz, so the total laser output bandwidth is 12 GHz.

4.5 Efficiency factors

The laser output efficiency is determined by a number of efficiency factors. By identifying these factors we can obtain a much better understanding of the diode-pumping process. The overall "wall plug" efficiency η can be written as the product of the individual efficiency factors:

$$\eta = \eta_D \eta_S \eta_C \eta_Q \eta_T \eta_E \,. \tag{4.12}$$

These factors are described in more detail below.

4.5.1 Electrical-to-optical efficiency

η_D is the diode electrical-to-optical conversion efficiency. The total electrical power consumed by the diodes to produce 2 W of optical emission is 6.71 W, giving a value of 0.30 for η_D.

4.5.2 Stokes efficiency

η_S is the Stokes efficiency and given by the quantum defect. As noted above, this term is 0.76.

4.5.3 Geometric coupling efficiency

The geometric coupling efficiency factor η_C is a measure of the overlap between the resonator mode and the inversion profile created by the pump beam. The coupling efficiency is a weak function of the ratio of the pump power to the threshold pump power, and depends as well on the ratio of the pump mode waist to the resonator mode waist. Based on published[6] modeling, a waist ratio of ~0.5 and a pump power ratio of 50, the factor $\eta_C \approx 1$.

4.5.4 Laser quantum efficiency

η_Q is the laser quantum efficiency and represents the fraction of absorbed pump photons that produces upper laser level population. This term is reduced from unity by the presence of nonradiating "dark sites." The value for the laser quantum efficiency is not the same as the well-known fluorescence quantum efficiency, as stimulated emission rather than spontaneous emission dominates the production of 1.06-μm photons in the laser cavity. An estimate of the laser quantum efficiency can be obtained from the slope efficiency. The latter is given by

$$\eta_{\mathrm{SLOPE}} = \eta_S \eta_C \eta_Q \eta_L \,, \tag{4.13}$$

where η_L is the resonator loss term given by

$$\eta_L = \left(1 + \frac{L_s}{1-R}\right)^{-1}, \tag{4.14}$$

and L_s is the single pass resonator loss ($=L_r/2$). η_L can be evaluated from the values for L_s and R given above and is shown to be 0.98. η_Q is then 0.78.

4.5.5 Transfer efficiency

η_T is the transfer efficiency. It represents the fraction of pump photons emitted by the laser diode that is absorbed by the Nd:YAG rod. Thus, it is the product of the pump optical system transport efficiency and the rod absorption. Specifically, it includes the collimating lens collection efficiency (0.88), the transmission of the other lenses in the optical train (0.95) and the PBC (0.97), the pump light transmission of the coating on the exterior face of the Nd:YAG rod (0.96), and the fraction of pump flux that enters the laser rod that is absorbed. (The values indicated in parentheses are the measured efficiencies of the various components).

From its definition,

$$P_A = \eta_T P_D , \tag{4.15}$$

where P_A is the power absorbed by the rod, P_D is the power emitted by the laser diodes, and η_T can be written as

$$\eta_T = [1-\exp(-\alpha\ell)](1-r), \tag{4.16}$$

where r includes all transport losses (noted above) that occur between the diode and the rod. The term $(1-r)$ is obtained from the product of the pump optics transport efficiency and the rod coating transmission. From the above values, these two terms are 0.81 and 0.96, respectively, and $(1-r)$ is 0.78. As mentioned earlier, the absorption term $[1-\exp(-\alpha\ell)]$ is 0.98, so that $\eta_T = 0.76$.

4.5.6 Extraction efficiency

η_E is the extraction efficiency, which measures the fraction of the total available energy stored in the resonator that is extracted as laser output. The extraction efficiency is given by

$$\eta_E = \frac{T}{T+L_r} - \frac{T}{2g_o\ell} , \tag{4.17}$$

where T is the transmission of the output coupler. Using the previously determined values for the gain and loss parameters, $\eta_E = 0.95$.

4.5.7 Summary of efficiency factors

As noted, the terms shown in Eq. (4.12) are individual efficiency factors that determine the laser "wall plug" efficiency. The role of each in generating laser emission can be illustrated by following the sequence of events required to convert electrical power drawn by the diodes to 1.06-μm laser output. The diode converts current to optical emission at 808.5 nm (η_D). The photons are collected by the pump optics and transported to the rod where they are absorbed (η_T). A fraction of the absorbed photons populates the upper laser level (η_Q), but only a fraction of the excited ions are produced within the active volume of the gain element (η_C). And, a fraction of exited ions in the active volume is extracted by stimulated emission to produce laser output (η_E). Of course, we will need to factor the difference in energy between a pump photon and a laser photon (η_S).

From Eq. (4.17) it can be seen that η_E increases as either the round-trip loss decreases or the gain increases. The mirror transmission affects η_E as well, and the maximum η_E is achieved with the mirror transmission set to T_{opt}. In fact, Eq. (4.10) is obtained by differentiating Eq. (4.17) and setting the derivative to zero. As noted earlier in this section, the optimum mirror transmission and hence maximum η_E can be established for any given pump power level, thereby ensuring that the laser is operating efficiently.

Summarizing the efficiency factors, the wall plug efficiency can be calculated by

$$\eta = \eta_D \eta_S \eta_C \eta_Q \eta_T \eta_E = (0.3)(0.76)(1)(0.78)(0.76)(0.95) = 0.13. \quad (4.18)$$

The calculated value is in excellent agreement with the measured wall plug efficiency, which is 874 mW/6.71 W = 0.13.

4.6 Dependence of the laser output power on the diode wavelength

Temperature tuning of the laser diode was discussed in Chapter 3. Experimental data can best illustrate the impact of the diode wavelength on the laser output efficiency. A low-resolution absorption spectrum of the 1-cm Nd:YAG laser rod is shown in Fig. 4.3. The region illustrated corresponds to the general wavelength range for diode pumping. The peak at 808.5 nm is fairly sharp, and the nearest peak to the red is at 813 nm.

The diode junction temperature was adjusted while observing the Nd:YAG laser output. The pump power was kept constant during this measurement. The results are shown in Fig. 4.4, where the output power obtained by pumping the rod with a single diode is shown as a function of diode output wavelength (top scale) and diode housing temperature (lower scale). Superimposed on this trace is the expanded absorption spectrum of the Nd:YAG laser rod.

It can be seen that the output power is highly sensitive to the diode output wavelength. As the pump center wavelength is adjusted between the absorption peak at 808.5 nm and the local minimum at 811 nm, the output power drops by 30%. As the diode output wavelength continues to increase, it eventually matches the absorption line at 813 nm and the 1.06-μm output power partially recovers. However, when pumped at this wavelength, the power is only 85% of the peak power.

This observed sensitivity is due primarily to the optical alignment required for efficient end pumping. Since the pump light is focused with a high-NA lens, it diverges rapidly after passing through a focus in the rod. After propagating several millimeters in the gain medium, the pump light diverges outside of the TEM_{00} mode volume. At a wavelength of 808.5 nm the absorption is high enough so that the pump beam energy is depleted as it passes beyond the active mode volume. However, at other pump wavelengths, a substantial fraction of the pump power remains in the beam as the "breakout" point is reached. This light is absorbed outside the active volume and is wasted, thereby reducing the overall pump efficiency.

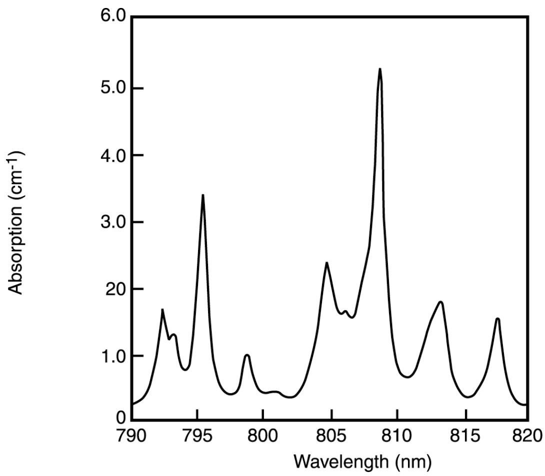

Figure 4.3. Low-resolution absorption spectrum of the 1-cm Nd:YAG rod.

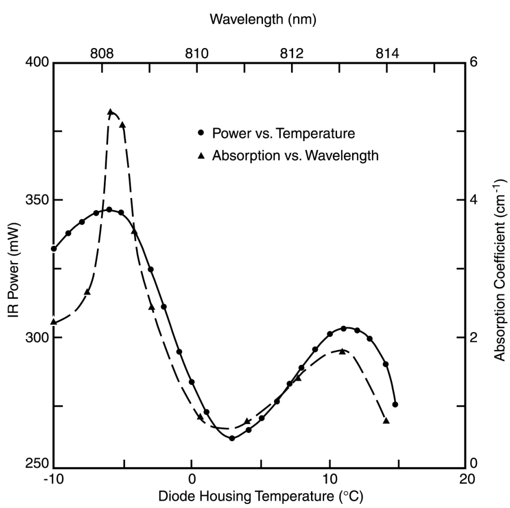

Figure 4.4. Dependence of the Nd:YAG laser output on the pump diode wavelength.

Part III

Advanced Concepts for Diode Pumping

Chapter 5

Power Scaling Considerations

Several aspects of power scaling have been addressed in previous sections. In this chapter, the basic issues involved with producing higher power from diode-pumped lasers will be covered in some detail. Before proceeding, however, it will be helpful to discuss the factors that are most prominent in the drive for more power.

There are three commercial lasers that account for much of the high-power laser sales, and diode-pumped lasers can in general replace them all. These are large frame argon ion lasers producing 20 W or more in the blue-green, Q-switched Nd:YAG lasers producing about 1 J/pulse at 1.06 μm with an average power of 10 W or greater, and cw Nd:YAG lasers producing 50 W or more in the IR.

Great strides have been made in producing both commercial and prototype diode-pumped lasers that are competitive with these products. For example, a 10-W cw 532-nm laser is currently available commercially, and higher-power, diffraction-limited TEM_{00} output is inevitable. Granted that a doubled Nd:YAG laser cannot do everything an argon ion laser can (the multiple-wavelength output of the latter, which includes the UV, is an important property for many end users), but for anyone who has had to deal with installing the utilities for a large-frame ion laser, the advantages of diode pumping are quite compelling.

For IR emission, both pulsed and cw diode-pumped lasers have been demonstrated at power levels comparable to commercial lamp-pumped devices. Output energies exceeding 1 J/pulse with repetition rates of hundreds of hertz have already been produced. Continuous-wave operation at 1 μm with output power exceeding 100 W has also been demonstrated, in both Nd- and Yb-doped materials. The problem that commercial manufacturers of diode-pumped lasers face is—and will continue to be—the component cost. Lamps are cheap; diodes are not.

An area that shows great promise for diode-pumped lasers is third and fourth harmonic generation of the 1.06-μm output of Nd:YAG. The resulting short-wavelength radiation is useful in semiconductor processing and photolithography. Output is typically TEM_{00} and may be cw or repetitively Q-switched. Harmonic generation from single-longitudinal-mode lasers has been demonstrated with high conversion efficiency at moderate power levels. Since throughput for industrial processing is dependent on output power, scaling is important for these types of lasers as well.

5.1 Scaling the diode pump power

We have previously discussed the advantages and limitations of both end-pumped and side-pumped geometries. In the context of power scaling there are some additional points to be made. Power scaling a diode-pumped laser starts by providing more pump power. So the discussion begins with a look at the issues related to scaling the diode output power.

Consider first the single-stripe diode, which may be either a stand-alone pump source or a building block for diode arrays. The power limitation for a single-stripe diode arises from the problem of facet damage. If the output power is too high, the diode facet will be permanently destroyed. Damage limits are generally given in terms of power density, but since the vertical dimension of most heterojunction diodes is identical, the power limit may be expressed as approximately 10 mW per micron of stripe width. Therefore, to produce more output power, the stripe must be made wider.*

However, there are limitations to increasing the stripe width. For one, if the stripe is too wide, the cavity mode has a tendency toward "filamentation," which means that the output is not uniform across the stripe. Instead, the laser emits in several narrow locations along the output aperture. While operation in this manner has numerous drawbacks for pumping, the most serious problem is that filamentation can damage the output facet. If the laser is operating near the damage limit (based on a uniform emission), condensing the full output power into several filaments produces "hot spots" at the mirrors and increases the risk of facet damage.

Commercial wide-stripe diodes have architectures that prevent filamentation, but the stripe cannot be arbitrarily wide. The "highest brightness" wide-stripe laser that is commercially available produces 1.2 W in a 100-μm-wide stripe, while single-stripe diodes emitting 4 W are manufactured with 500-μm-wide stripes.

A second problem for producing wide-stripe diodes is the possibility of ASE in the direction transverse to the laser axis. Since laser diodes are typically 300 μm long, a laser with a stripe-width dimension comparable to the cavity length can exhibit serious losses due to ASE. While the device architecture can be designed to minimize these losses, ASE will impose an additional limitation to diode stripe width scaling.

A third limitation is that as the diode stripe widths increase, the output across the aperture becomes less coherent. At a certain point there is little difference between a single superwide-stripe diode and a diode array.

5.1.1 Diode arrays

There are two types of arrays: qcw and cw. The 1-cm linear array is the most powerful single component for diode pumping. The bar consists of multiple

* This corresponds to 1 MW/cm^2 for a 1-μm-thick junction. This output power scaling is a guide for contemporary commercially available laser diodes, which are generally limited by facet damage. Damage begins to occur at several megawatts per square centimeter, but high-quality semiconductor material can withstand densitites as high as 200 MW/cm^2.

individual stripes located on a single GaAs substrate. The individual diodes share the same heat sink, are powered by a single electrical lead, and because they are produced from the same part of the wafer have similar (but not identical) wavelengths. An illustration of a linear array is shown in Fig. 5.1.

A fundamental constraint for diode array operation is related to the problem of heat removal. A single-stripe diode operates in an environment where there are no additional sources of heat. Therefore, heat removal takes place in both the horizontal and vertical planes. With arrays, however, each diode is adjacent to another diode and the only effective route for heat removal is in the vertical plane. The reason that qcw arrays were developed before cw arrays is the thermal problem. The stripes on both types of arrays are similar, but with a duty factor as low as 1%, the heat load is far more manageable than for a cw array.

The breakthrough for thermal management arrived with microchannel cooling. In this geometry cooling fluid is circulated close to the active layer. The fluid flows through capillary-size conduits located near to, and sometimes within, the substrate. This type of cooling is used for cw as well as qcw arrays. Higher duty factors or more output power can be produced from arrays with effective cooling. It is useful to note that liquid coolant is not required for commercial arrays producing less than 50 W cw. These devices are cooled thermoelectrically using Peltier coolers.

The considerations for scaling the output power of a diode array are somewhat different than that for a single-stripe diode. Currently, cw arrays are composed of a series of 1-W, approximately 100-μm-wide stripe diodes on a 1-cm bar. The diode array output power is determined by the packing density. Thus, a 10-W array has 10 stripes for a 10% packing density, while a 20-W array will have a 20% packing density. Quasi-continuous-wave arrays can have packing densities as high as 96%. They are fabricated using 1-W laser diodes with stripe widths just under 100 μm. The 100-W 1% duty factor bar currently produces the highest pulsed output power for a qcw array. Higher duty factors are available at reduced output power. For power outputs higher than 100 W, 2D "stacks" of bars are used. Power levels up to 5 kW are currently offered.

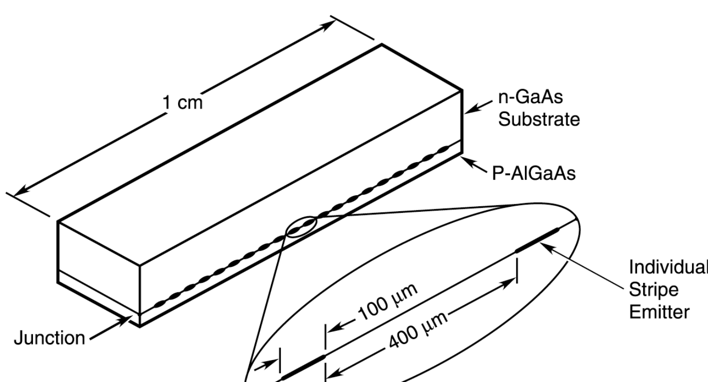

Figure 5.1 Schematic of a 1-cm diode array with a 20% packing density.

The scaling issues associated with fiber-coupled arrays are similar to those for cw arrays, although the possibility of damage to the fiber core must be considered as well. The 20-W cw laser contains 20 diodes, each with an emitting aperture of 100 μm. The fiber core for each stripe is about 100 μm as well, so the power density in the fiber is substantially below that in the diode laser cavity (the intracavity power for the diode is higher than the emitted power, and the diode emission aperture is rectangular). Therefore, optical damage to the fiber is not usually an issue, but it can become one if the diode output were focused onto a smaller core fiber. The diameter of the fiber bundle for the commercially available 20-W array is 600 μm.

Scaling end-pumped lasers requires different considerations than for side-pumped designs, as was noted previously. To the extent that scaling is simply a matter of obtaining higher-power pump diodes we can get comparable cw power suitable for either pump geometry (50–65 W per bar). The difference is that the fiber-coupled bar is more than three times as expensive as the bare bar. Multiple linear arrays can be used for either pump method, although with end pumping, unique geometries are required to allow pumping with more than two arrays.

However, scaling is not only a matter of pumping harder. The high pump power density associated with end pumping, which is an advantage for providing low-threshold, high-efficiency TEM_{00} output power, becomes a limitation for scaling. High power densities produce undesirable thermal effects. If compensation is provided by expanding the pump and resonator mode diameters (to maintain a constant pump power density), the gain aperture may be lost. This will produce multimode operation. Similarly, scaling a side-pumped geometry by pumping with more arrays exacerbates the tendency for this type of pumping to produce multimode operation. In this section, two designs will be discussed for end-pumped lasers that exceed the 874-mW output that was produced by the device designed in Chapter 3.

5.2 Thermal effects

5.2.1 Thermal lensing

There are numerous thermal problems associated with power scaling. Refractive index variations created by nonuniform energy deposition distort the optical path through the gain medium. This distortion can produce several undesirable effects, and various techniques have been developed to compensate for them. One common problem is thermal lensing. This produces a generally weak lens in the rod, which in turn alters the resonator mode. For a rod uniformly side-pumped along its length, the thermal lens focal length is given by

$$f = 2KA_{\mathrm{p}}[P_{\mathrm{h}}(dn/dt)]^{-1} \tag{5.1}$$

where f is the focal length of the thermal lens, K is the thermal conductivity of the rod, A_{p} is the pump mode area. P_{h} is the fraction of the pump power converted to heat, and *dn/dt* is the thermal coefficient of the index of refraction. The lens gets worse (i.e., the focal length gets shorter) as the pump power density (power per unit area) increases. Note that the thermal deposition profile is assumed to be cylindrically symmetric.

5.2.2 Other thermal effects

There are a number of other thermally induced phenomena that affect laser operation. Thermal fracture is one, caused by the different coefficients of expansion along the rod axes. Nonuniform heating by the pump fluence produces stress which may produce fracture as well. Optical distortion is created when thermal gradients develop across the emitting aperture. Mild distortion affects the beam quality, while severe distortion can terminate laser operation. Distortion can also be produced as a result of nonuniform thermal expansion of the gain medium.

Thermal birefringence is a problem produced by the mechanical strain that develops from thermal gradients. The hotter central region of the rod is constrained from expansion by the cooler, unpumped part of the rod. Thermal strain produces refractive index variations along certain directions in the rod, creating birefringence. Induced birefringence will partially depolarize linearly polarized light passing through the laser rod. A number of modes of laser operation require a linearly polarized beam, including *Q*-switching and intracavity SHG. Thermally induced birefringence has the potential for introducing significant depolarization losses. To see this, note that generating polarized light in an isotropic Nd:YAG laser requires the insertion of polarization-sensitive losses. As birefringence depolarizes the light, the internal losses increase and the output power will drop. This may be accompanied by beam distortion as well.

Scaling end-pumped lasers will introduce undesirable thermal effects at lower pump power levels than when scaling side-pumped lasers. As noted above, this is due to the higher pump power density used in end pumping. In either case, however, thermal problems will begin to become significant above 2 to 3 W of laser output.

5.3 Novel designs for end pumping

In general, there are two ways to scale an end-pumped laser. One is to provide more pump power in a manner consistent with end pumping (i.e., from a single aperture). The other is to provide a gain element design that allows end pumping along more than one axis. Means for providing more pump power have been discussed previously; these include fiber-coupled linear arrays and light ducts. In addition, end-pumped designs have been reported that incorporate imaging of the linear array using discrete optics. These beam control methods allow efficient end-pumping with a 1-cm-long linear array.

The most interesting end-pumped scaling concepts allow pumping along more than one axis, as this distributes the thermal heat load and reduces the impact of the thermal effects discussed above. Two such designs are reviewed below.

5.3.1 Penta-prism

The penta-prism laser is an example of a class of internally folded[7] laser gain elements that can be efficiently end pumped. The laser is shown in Fig. 5.2, where the size of the gain element relative to the resonator length is exaggerated to illustrate the multiple pump axes. By "folding" the resonator mode axis by reflections from two of the prism faces, a total of five pump axes can be provided. Three pump axes were used to demonstrate this laser and are labeled 1, 2, and 3 in the figure. The other two axes are labeled "pump." The resonator mode is nearly hemispherical, with a waist formed on the face labeled C. The dimensions of the penta-prism are small—the orthogonal sides are only 5 mm long. This means that the mode diameter does not expand significantly as it traverses the penta-prism. In fact, comparable threshold power and slope efficiency are achieved when the prism is pumped along any of the axes shown.

Because each fold face is accessible for end pumping (in this case, "longitudinal pumping" might be a more appropriate term) short-focal-length, high-NA focusing lenses can be used. This is not true for "two-sided" end pumping, where one attempts to pump the interior face of the rod through a discrete fold mirror. Another important feature of the design is that the pairs of pump axes at fold faces A and B are almost orthogonal with respect to one another. This produces good access to the four pump directions at the fold faces while allowing the use of off-the-shelf macroscopic lenses.

An important feature of this design, noted above, is that heat deposition along each of the pump directions is located in a separate volume. Thus, thermal effects are diminished relative to what they would be if all of the pump power were

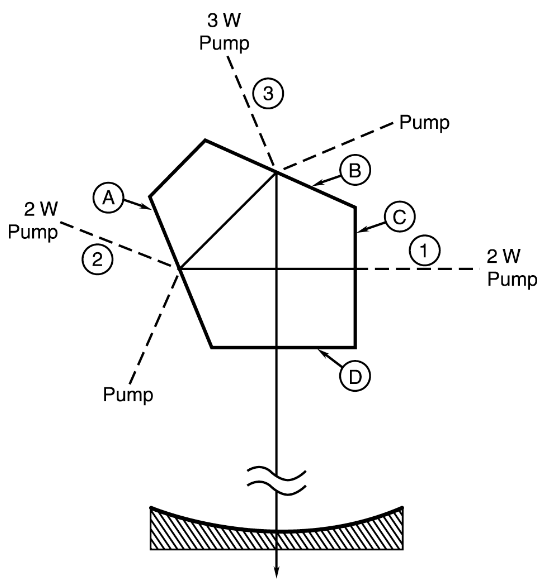

Figure 5.2. Resonator and pump axes for the end-pumped penta-prism laser.

deposited along a single axis. The threshold and slope efficiency for the penta-prism laser are excellent, comparable to those obtained for the laser designed in Chapter 3 (shown in Fig. 4.2). This design produced 2.3 W of output power at 1.06 μm. The penta-prism performance is illustrated in Fig. 5.3.

5.3.2 Diode-pumped ring laser

Another approach for providing multiple pump axes is shown in Fig. 5.4. In this design the resonator mode is reflected from the exterior surface of the Nd:YAG rod. This face is oriented so that the angle of incidence of the resonator with the interior face of the Nd:YAG crystal is equal to Brewster's angle. The mode waist is located at the exterior face. Thus, longitudinal pumping can be provided along two axes as shown. The use of Brewster's angle helps to maintain the proper polarization orientation of the intracavity flux, which is important for unidirectional operation. A useful by-product of this large angle is that the two pump axes are separated by more than 120°, greatly facilitating the simultaneous use of both axes.

Referring to Fig. 5.4, two versions of the ring laser are shown. The upper schematic illustrates the basic ring laser. In this version the mode contained between the two fold mirrors is collimated. The lower schematic shows the ring configured to produce repetitively *Q*-switched, SHG emission. Here the mode comes to a focus between the two fold mirrors. The chopper provides 3-KHz repetition rates with no insertion loss.

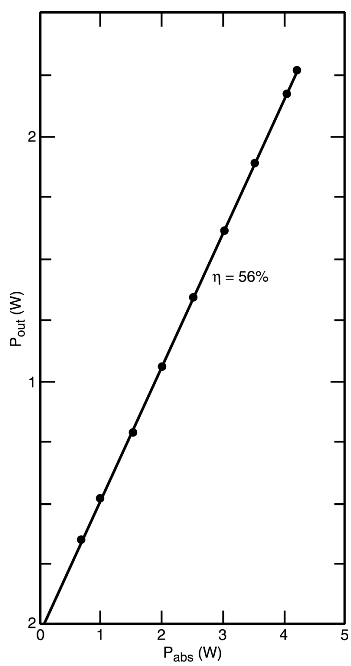

Figure 5.3. Dependence of the penta-prism laser output power on pump power.

The performance characteristics of this diode-pumped unidirectional ring laser are presented in Chapter 10.

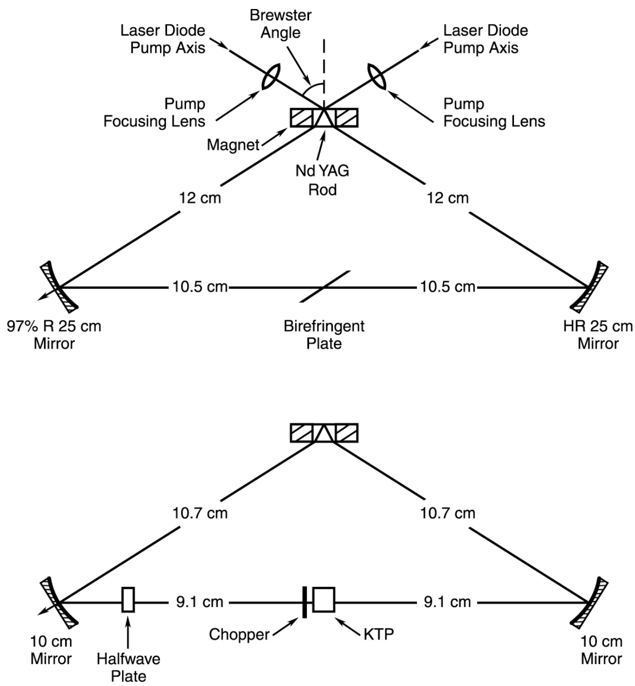

Figure 5.4. Configuration of a unidirectional ring laser with two longitudinal pump axes.

5.4 Fiber-coupled laser diode arrays: Power density

One aspect of fiber-coupled arrays as it relates to the scaling of end-pumped lasers is the pump power density. Simply increasing the pump power will not produce more laser power with the same high efficiency. The pump power density must be maintained. A currently available high-brightness cw fiber-coupled array produces 16 W in a 600-μm-diameter fiber bundle. The average pump power density is 5.7 kW/cm^2. For a laser diode, the high-brightness device produces 1.2 W in a 100×1 μm^2, so the power density is 1.2×10^6 W/cm^2. Thus, 200 times higher pump power densities can be obtained with a 1.2-W diode than with the 16-W fiber-coupled array. By scaling up the pump power at a reduced power density, the device performance will be characterized by higher threshold, lower gain, and lower slope efficiency. However, the spot size produced by the fiber can be reduced by using focusing optics. This will increase the power density but increase the pump divergence in the rod as well.

5.5 Spectral bandwidth of diode arrays

Broad-stripe laser diodes (stripe widths greater than a few microns) typically have bandwidths of 1 to 2 nm. Continuous-wave linear arrays have bandwidths that are convolutions of the bandwidths of each individual stripe on the diode array. As a consequence, the emission bandwidth of a high-power linear array is somewhat larger. These arrays have specified bandwidths that fall in the range of 2 to 4 nm.

Chapter 6

Side-pumped Designs

Efficient side pumping is produced by following the same general guidelines as for end pumping. For either geometry, the best efficiency is achieved by depositing the maximum amount of pump energy within the TEM_{00} mode volume. The pump and mode waist trade-offs are identical insofar as they affect the gain, threshold, slope efficiency, and thermal issues. However, one important difference in this regard is that with side pumping, a small pump waist can be produced over a larger axial range than with end pumping. This reduces thermal effects. To see this, imagine the classic side-pumped dye laser or dye amplifier. Recall that in this arrangement, a laser pump beam from a doubled Nd:YAG or other source is focused with a cylindrical lens onto the side of a dye cell. The focus forms a horizontal line near the cell wall as viewed from the pump laser propagation direction. However, from the direction of the dye laser optical axis, the active volume appears cylindrical; and, in fact, it forms a gain aperture. The dye concentration is adjusted to prevent penetration of the pump beam much beyond the diameter of the resonator mode volume within the cell.

Note, however, that the pump power density is lower than it would be if the pump laser output had been focused with a spherical lens. Thus, for the same pump power, the gain will be lower. But thermal effects, which are problematic at higher laser operating power, remain controllable in a side-pumped geometry. In addition, for scaling purposes, somewhat higher cw power is available (diode-to-fiber coupling losses are about 20%); and, more importantly, linear arrays can be used for side pumping without fiber coupling or sophisticated optics. This greatly lowers the cost per watt of diode pump power.

Unlike lamp pumping, where imaging is difficult and the spectral bandwidths are broad, side pumping with laser diodes allows the use of more controlled, better-directed pump excitation. Some modern side-pumped designs are variations of the side-pumped dye laser geometry discussed above. That is, the resonator mode is produced near the outer edge of the gain element, where the combination of pump wavelength and doping density are adjusted to produce relatively efficient TEM_{00} output. This type of side-pumped design is preferred when pumping with a single linear array, for which tens of watts of cw or qcw output power can be produced. When higher pump power is needed, this type of design can be used in conjunction with a lens duct, for example. A 2D diode array can be compressed in the vertical dimension with appropriate ducting to deliver suitably tailored pump power. An alternative approach that is particularly useful when multimode operation is acceptable is to simply surround the laser rod with several bars and focus the output into the center of the rod using cylindrical optics.

The range of side-pumped geometries is far too extensive to treat in detail in this text. As the discussion of end pumping was limited to two designs, the same will be done with side pumping. The major point to be made is that when selecting a pump geometry, the factors that should be considered are those that affect the laser parameters (gain, threshold, slope efficiency), thermal effects, and the overall cost budget for the laser. From the preceding sections the reader should have a sufficient understanding of the appropriate trade-offs for a given operating power level. The application may play an important role in the selection of the pump geometry as well.

6.1 Zig-zag slab laser

The zig-zag slab laser was developed several decades ago to produce high beam quality output from solid state lasers that were severely distorted by nonuniform gain. The gain medium is fabricated in the shape of a thin rectangular solid ("slab") with the long edges perfectly parallel. These are the faces that receive the pump light. The energy deposition and hence gain profile in the slab varies exponentially with increasing distance from each pumped face. By designing the resonator optical axis so that it "zig-zags" between the two parallel pumped faces of the slab, the mode integrates over the spatial variations of both the gain profile and the thermal distortions induced by the pump. This results in a more uniform output beam.

A diode-pumped commercial version of the slab laser was produced in the early 1990s. The laser is side pumped and was termed "TFR," for tightly folded resonator. This design approach allowed the manufacturer (Spectra-Physics) to take advantage of the then newly developed 1-cm linear arrays. The TFR produced the highest laser output power commercially available at the time; it is illustrated in Fig. 6.1.

The laser resonator is aligned so that each bounce point in the slab corresponds to the location of a laser diode stripe on the diode array. The diode array output is collected and collimated in the fast axis with cylindrical optics. Using an array with 10 stripes, the laser resonator was designed to contain 10 bounce points in the slab. The TFR can be thought of as a multi-end-pumped laser, where each diode on the array pumps along a separate axis. This is not quite as efficient as true end pumping, since the pump power density produced by each stripe is not nearly as high in this geometry as when the diode output is focused with a spherical lens. In addition, while the design allows the natural divergence of the pump beam in the horizontal plane to overlap the folded pair of resonator axes at each bounce point, the pump light axis is not exactly coincident with the resonator axis, and a significant fraction of the light is absorbed outside of the active volume.

The TFR made quite an impact when first introduced in the marketplace. This laser produced more than 2 W of output power at 1.06 μm during the period of time when commercial devices from other manufacturers were producing tens of milliwatts.

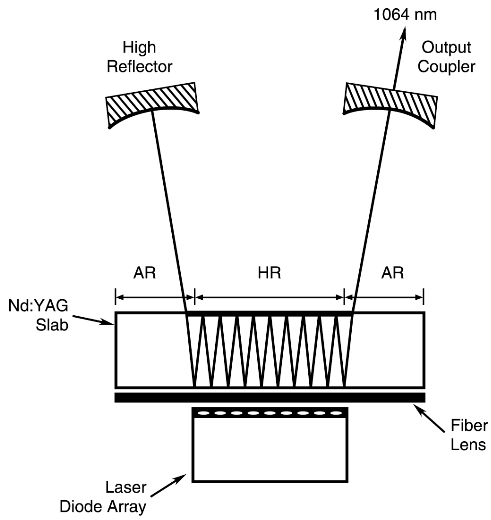

Figure 6.1. Commercial TFR laser.

6.2 Novel side-pumped design

A more traditional but novel side-pumped laser design is illustrated in Fig. 6.2. This design incorporates three of the side-pumped dye laser concepts discussed above. First, the resonator mode is located near the pumped face of the “rod” (which is rectangular in cross section). In addition, the pump laser diode array output is focused onto the rod with a cylindrical lens. This cylindrical lens is simply a bare fiber. Third, the absorption coefficient at the pump wavelength is quite large, maximizing the deposition of pump energy near the pumped face of the gain medium. This is accomplished by selecting vanadate as the Nd ion host. As was presented in Chapter 3, vanadate has a very high extinction coefficient at the diode output wavelength. Since pump light does not penetrate deeply into the crystal in the direction transverse to the laser optical axis, the pump efficiency achieved with this design is quite high.

The unique feature of this design, and one that distinguishes it from the dye laser, is that the resonator mode is reflected at the pumped face. The reflection is due to TIR, so that it does not require a reflective coating. More importantly, however, the reflection has the effect of allowing the resonator mode to average out the inherently nonuniform transverse gain profile. Since the attenuation of the pump light is exponential along the pump propagation axis, the gain decreases with distance from the pumped face of the rod. Going from left to right in Fig. 6.2, the side of the resonator mode closer to the diode array experiences higher gain than the opposite side. However, upon reflection, the two sides of the mode reverse their position relative to the diode array, so that the side that had experienced lower gain prior to the bounce now experiences higher gain. Since the bounce point is centrally located with respect to the width of the diode array, the resonator mode may be considered as comprising complementary ray pairs, each ray in the pair being equidistant from the central resonator axis in the plane of incidence. Then, each of the two rays in each ray pair will experience the same amount of gain.

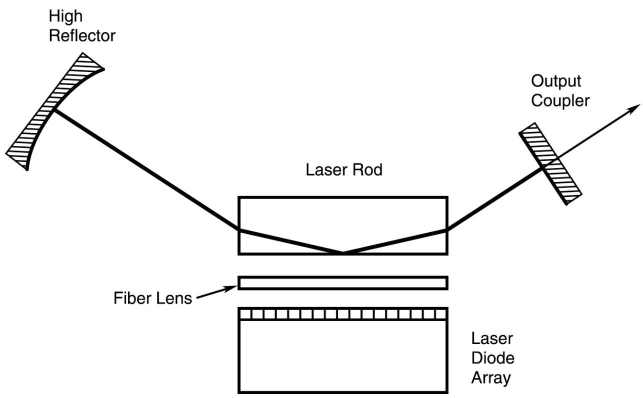

Figure 6.2. Grazing incidence slab laser.

With this pump geometry and resonator, more than 30% optical conversion efficiency and 44% slope efficiency were achieved.[8] More recent results with Nd:YVO_4 indicate more than 1 mJ of Q-switched output energy at a repetition rate of 1 kHz. A commercial product (Liconix) that uses a similar design produces up to 2 W of 355-nm output (third harmonic of Nd:YVO_4) at 20 kHz.

Chapter 7

Other Output Wavelengths for Nd-doped Lasers

The 1.06-μm transition in Nd:YAG is the most well known and widely used. However, as with many rare earth ions, the Nd ion has several electronic levels that can produce emission at other wavelengths. A partial energy level diagram for Nd:YAG is illustrated in Fig. 7.1. Two transitions have been diode-pumped and are of interest for several applications. They are the 1.3-μm and the 946-nm transitions. Diode-pumped laser operation at these two wavelengths is discussed briefly in this section.

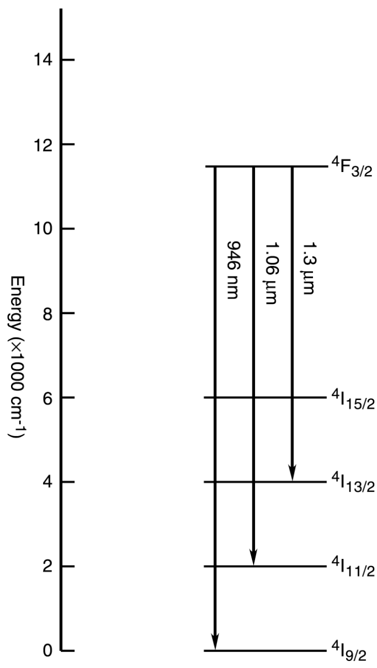

Figure 7.1. Partial energy level diagram for Nd:YAG showing the major laser transitions.

7.1 Operation at 1.3 μm

The 1.3-μm wavelength is produced by the ${}^4F_{3/2} \rightarrow {}^4I_{13/2}$ transition. It involves the same upper laser level as the 1.06-μm transition and therefore can be pumped using the same diode wavelength. Operation at 1.3 μm is of interest for certain fiber communications applications, as well as for red wavelength generation using nonlinear optics. There are two main 1.3-μm transitions in Nd:YAG, each involving a different Stark level. The line with the lower threshold is at 1.319 μm, while the other operates at 1.338 μm.

Production of laser emission at 1.3 μm is different in several ways than at 1.06 μm. For one, this transition is less efficient. The threshold is about 60% higher for the 1.319-μm line, while only about half as much output is produced at 1.3 μm than would be generated at 1.06 μm for the same pump power. The stimulated emission coefficient in Nd:YAG is only about one-sixth that of the 1.06-μm line, so at high pump power ASE has the potential to introduce significant losses. Finally, the Stokes efficiency for this transition is lower—0.61 compared to 0.76. Therefore, a larger fraction of the pump fluence deposited in the rod generates waste heat, and thermal effects will be more severe than for the 1.06-μm transition when pumping with the same power density.

Operation at 1.3 μm may be enhanced by using host crystals other than YAG. For many years YALO has been used for laser emission at 1.3 μm. With the proper crystal orientation, the cross section at 1.3 μm in YALO is comparable to that at 1.06 μm. This lowers the potential for losses introduced by ASE, particularly for *Q*-switched operation. Vanadate has advantages for 1.3-μm operation as well and is more readily available than YALO. With this crystal, the stimulated emission cross-section ratio is 1:4, which is somewhat improved compared to Nd:YAG. However, the magnitude of the stimulated emission cross section at 1.3 μm is more than two times higher than that of Nd:YAG at 1.06 μm!

This transition has been demonstrated using many different resonator configurations, and numerous diode-pumped 1.3-μm lasers are commercially available, including the TFR (Spectra-Physics), a unidirectional ring (Lightwave MISER), and several traditional end-pumped designs.

7.2 Operation at 946 nm

The 946-nm transition is a difficult one to work with, as the terminal level is the ground state. The transition that produces this wavelength is $^4F_{3/2} \rightarrow {}^4I_{9/2}$, and several problems arise from the fact that the laser is essentially three-level. Reabsorption loss due to ground-state ions can be significant and drives the design parameters.

This laser has been the subject of a good deal of activity, as the second harmonic wavelength is at 473 nm. Over the years, numerous applications have materialized that require a high-power blue solid state laser. Diode pumping has been demonstrated by several researchers, some producing well over 1 W at 946 nm. One of the many problems introduced by reabsorption loss is that the end-pumped laser design constraints will allow the most efficient operation at only one pump power level and hence at a fixed output power. That is, as the laser rod length is designed to minimize reabsorption losses at full pump power, the losses increase when the diode output power is reduced. Reabsorption losses are dynamic, being reduced as the ground state is partially depleted. The efficiency of this transition is also temperature sensitive since the steady-state population in the terminal laser level, which is an excited Stark level of the ground state, is determined by the Boltzmann distribution. Despite these problems, lasers operating at this wavelength have been demonstrated with power levels that are greater than 40% of the 1.06-μm output power.

The 946-nm laser is difficult to end pump because unexcited Nd ions in the active volume produce loss. In a traditional end-pumped laser, the rod length is designed to absorb most of the pump flux, and therefore the “tail” end of the rod sees little or no excitation. For 946-nm operation, the unexcited end of the rod will introduce reabsorption loss. The requirement for end pumping is therefore that the rod length remain short enough so that substantial pump flux propagates to the end of the rod. This means that a non-negligible fraction of the pump light will exit the rod and the pump efficiency will be diminished. In some designs, the transmitted pump light is reflected back through the rod for a second pass.

Side pumping poses a different set of design constraints. For one, the pump power density is generally lower, so the population of ground-state absorbers is higher for a given pump power than it would be under end pumping. A second problem is that side-pumped rods are usually held in “collars” at each end. The collars allow better cooling of the rod, which is particularly important for three-level lasers since the inversion is temperature-dependent. But this brings about serious problems for the 946-nm transition, since the region of the rod shaded by the collars is unexcited and hence produces reabsorption loss. One solution to this problem has been to use undoped YAG end caps that are diffusion bonded to each face of the rod. These end caps provide a region for the collars to make good thermal contact but do not absorb the 946-nm light.

Chapter 8

Diodes for Pumping Other Gain Elements

As noted previously, AlGaAs diodes operate between approximately 725 nm and 850 nm, depending on the Al content in the active layer. There are other gain elements whose excitation wavelengths are outside of this range. In this chapter we will briefly discuss two other types of laser diodes.

8.1 900-nm diodes

By replacing Ga in GaAs with In, the diode wavelength increases. This is the opposite of what occurs when Al replaces Ga. The major thrust for developing InGaAs laser diodes is that Er-doped fiber amplifiers require 980-nm excitation. Currently, 60-W qcw linear arrays, 40-W cw arrays, and 4-W 100-μm-stripe InGaAs diodes are commercially available. The approximate output wavelength range is from 910 nm to 980 nm. As InGaAs diodes are required for pumping Yb-doped crystals, it is inevitable that a wider range of these diodes will be produced in the future.

8.2 670-nm diodes

These diodes, referred to as "visible" laser diodes, are composed of AlGaInP. They are termed "quaternary" (the diodes discussed previously are "tertiary") because the active layer contains four elements. One of the problems faced by manufacturers of these diodes is the use of phosphorous in the MOCVD process. This element poses numerous safety hazards. In addition, the MOCVD facility for making phosphorous-based diodes must be a dedicated one, tying up a substantial amount of capital for the production of limited types of semiconductors.

There are numerous uses for these diodes since they operate over a wide (and popular) wavelength range. The long wavelength cutoff is about 690 nm, while at the short end they have been demonstrated below 600 nm. Commercially, it is difficult to obtain diodes below 660 nm, although their use as a replacement for HeNe lasers in bar code scanners continues to drive research at the short-wavelength end. Diode lifetime below 660 nm is a major problem—the active layer composition is not receptive to operating for long times at these wavelengths.

Aside from bar code scanners, several medical applications such as photodynamic therapy make these diodes useful. Since Cr^{3+} ions absorb strongly in the red, visible laser diodes are particularly useful for diode pumping. Cr-doped lasers will be discussed in more detail in Chapter 9.

Currently, 0.5-W, cw, 250-μm-wide stripe devices are available, as are 3-W fiber-coupled arrays. Several manufacturers supply visible laser diodes.

Chapter 9

Examples of Other Diode-pumped Lasers

In this chapter, the operation of Yb-doped crystal lasers, tunable Cr^{3+} doped lasers, and dye lasers is reviewed.

9.1 Yb-doped Lasers

Yb^{3+} is a rare-earth ion that has demonstrated lasing in a number of crystalline and glass hosts. It has several important features that are particularly useful for diode-pumped operation. For one, it is unique among rare-earth ions in that it has only one excited state. This allows high Yb^{3+} doping densities to be used without the usual concerns about concentration quenching, which is useful for designing compact diode-pumped lasers. The gain element can be configured as a disk, for example, with an absorption pathlength of less than a millimeter. Yb^{3+} has two intense absorption bands located near 940 nm and 970 nm, and can be pumped by InGaAs laser diodes. Yb^{3+} is often used as a co-dopant as well, and has been particularly effective in upconversion lasers.

The peak laser emission wavelength for Yb^{3+} is 1.03 μm. This wavelength is close to the 950-nm pump diode wavelength, and it produces a Stokes efficiency exceeding 0.9. In addition, Yb lifetimes are relatively long. In Yb:FAP (FAP is fluoro-apatite), for example, the lifetime is 1.8 ms. Recalling the previous discussion regarding the advantages of Nd:YLF for *Q*-switched operation due to its 480-μs lifetime, it can be seen that there is an important cost advantage in using Yb-doped crystals for low-repetition-rate, high-energy lasers. For example, a 100-W qcw bar produces 10 mJ per 100 μs of pulse operation. For Nd:YAG, this corresponds to a deposition of 23 mJ of pump energy per pulse for an excitation pulse width equal to the fluorescence lifetime of 230 μs. For Yb:FAP, on the other hand, the 100-W diode array will deposit 180 mJ in the crystal for an excitation pulse width equal to the fluorescence lifetime. Therefore, to produce a 1 J per pulse Yb:FAP laser, assuming the previously used 35% optical conversion efficiency, would require a diode pump power of only 1.6 kW, compared to the 12-kW array that is required to produce the same output energy in Nd:YAG. Put in terms of cost, for Nd:YAG one needs 124 of the 100-W arrays to produce the 1-J output, while for Yb:FAP only 16 arrays are required. This reduces the pump cost by the price of 108 arrays (about $100,000 at current prices).

A problem for the Yb:FAP laser is that with 1% duty-factor qcw arrays, operation is limited to repetition rates of about 5 Hz. A nominal 10-Hz laser would require diode arrays with a 2% duty factor, while a 20% duty factor diode array will produce repetition rates of 100 Hz. Another issue related to Yb is that it operates as a three-level laser. Therefore, reabsorption loss and temperature control of the gain medium are important for this ion. In spite of this, however, great success has been demonstrated with diode-pumped Yb-doped lasers. For example, several years ago (February 1998) it was reported that cw operation of a Yb:YAG laser produced power levels of approximately 1 kW multimode. The diode pump wavelength was 940 nm. The excited-state lifetime of Yb in YAG is about 1.2 ms.

9.2 Cr-doped tunable solid state lasers

More than two decades have passed since the alexandrite laser was first demonstrated. Alexandrite is Cr^{3+}-doped chrysoberyl ($BeAl_2O_4$), and it produces tunable laser emission over the range of 720 nm to 800 nm. For about 10 years after alexandrite was demonstrated, there was little noteworthy research in tunable solid state lasers. Then, the Ti:sapphire laser was introduced, initiating a resurgence of interest in tunable near-IR lasers. Several years later, Lawrence Livermore National Labs announced success with several Cr-doped colquiriite tunable lasers, including Cr:LiCAF and Cr:LiSAF. This development, in conjunction with advances in AlGaInP diode production, was instrumental in bringing about the current interest in diode-pumped tunable Cr-doped lasers.

While several Cr-doped laser crystals have been developed, Cr:LiSAF has generated the most interest. This laser has a tuning range that competes with Ti:sapphire, operating from about 770 nm to 1 μm. But much of the interest in this material stems from its ability to be diode-pumped. Cr^{3+}-doped lasers are pumped with visible laser diodes, while Ti:sapphire cannot be directly diode-pumped with currently available diodes. Most cw and many pulsed modes of operation of the Ti:sapphire laser (including ultrashort pulse emission) use an argon ion laser for the pump source. For many modes of operation, the Ti:sapphire performance parameters can be duplicated and produced more efficiently with a diode-pumped Cr:LiSAF laser.

An important feature of colquiriite crystals for diode pumping is that the absorption coefficient is not strongly dependent on polarization. This enables efficient pumping using polarization combination of laser diodes or fiber-coupled visible laser diode arrays that use standard non-polarization-preserving fibers. This is not the case for alexandrite, where only one orientation of the pump polarization is absorbed effectively.

A second advantage for diode pumping is that the Cr^{3+} absorption bandwidth is enormous compared to rare-earth ions such as Nd. In fact, while for Nd the absorption bandwidth is only a fraction of the range of wavelengths accessible by AlGaAs diodes, the opposite is true for Cr-doped lasers. That is, the range of wavelengths available for AlGaInP laser diodes is only a fraction of the Cr^{3+} absorption bandwidth. The colquiriite crystals have absorption peaks near the wavelength range where visible laser diodes are most readily available. The absorption spectrum of Cr:LiCAF is shown in Fig. 9.1. For comparison, alexandrite has an absorption peak at a significantly shorter wavelength (near 600 nm).

One of the problems for diode-pumped Cr-doped lasers is that the gain cross sections are low compared to Nd:YAG (1×10^{-20} cm^2 for Cr:LiCAF, 5×10^{-20} cm^2 for Cr:LiSAF). This means that the gain for a given pump intensity will be lower. As a consequence, more care must be taken when diode pumping to produce high pump intensities in the crystal. Cr-doped laser performance is more sensitive to the brightness of wide-stripe diodes, as well as to the lower pump intensity produced by fiber-coupled visible laser diode arrays. The best results for visible diode pumping using linear arrays will be obtained with micro-lens assemblies.

An example of one of the diverse applications of visible laser diode pumping is the co-doped Cr,Nd:GSGG laser. This crystal was developed originally for flashlamp pumping to take advantage of the broad spectral absorption of Cr^{3+}. The Nd ion absorption spectrum consists of several narrow groups of lines, while the flashlamp emission spectrum is that of an approximately 10,000°K blackbody. Therefore, flashlamp pumping Nd-doped crystals results in significant amounts of pump energy not being absorbed. On the other hand, Cr^{3+} ions have broad absorption bands in the red, blue, and near-UV. The transfer efficiency between an excited Cr^{3+} ion and the $^4F_{3/2}$ upper laser level of Nd is almost 90% in GSGG. It was found early on that co-doped, flashlamp-pumped Nd lasers were significantly more efficient than singly doped lasers.

How is this related to diode-pumping? As discussed in Chapter 4, diode-pumped Nd-doped laser efficiencies are sensitive to the central wavelength and bandwidth of the pump diodes. This creates several problems in the laser design and adds to the overall cost, both in terms of diode wavelength selection and the requirements for temperature tuning. These problems can be avoided by using visible laser diodes to pump codoped GSGG. Initial results for a visible laser diode-pumped Cr,Nd:GSGG show high-efficiency 1.06-μm operation that is remarkably insensitive to pump wavelength. In addition, the laser demonstrated extremely low threshold power—about 930 μW when pumped at 670 nm.

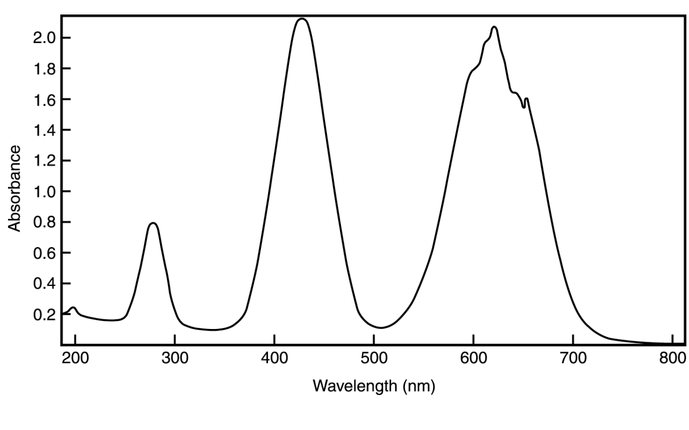

Figure 9.1. Absorption spectrum of Cr:LiCAF.

9.3 Dye lasers

Another area where pumping with visible laser diodes has made an impact is as an excitation source for cw dye lasers. Dyes that absorb in the 650- to 700-nm range are typically pumped by krypton ion lasers. The krypton laser has all of the drawbacks of an argon ion laser (low efficiency, high cost, expensive utilities, excessive weight and volume), but it is also less versatile. That is, the 650-nm krypton output has far fewer uses than the shorter wavelength emission from an argon laser. As a consequence, krypton lasers are not commonly available.

On the other hand, tunable dye lasers that emit in the 700- to 800-nm range have a number of applications. Since laser diodes producing 0.5 W of visible emission are available and far more convenient to use than krypton ion laser, the development of a diode-pumped cw dye laser has substantial appeal.

Several different diode-pumped dye lasers have been demonstrated[9] using a polarization-combined pair of visible laser diodes. The resonator and pump optics are shown in Fig. 9.2. The pump dye laser was used to demonstrate power scaling, as the laser diode power used for the measurements was limited. The resonator configuration is nearly hemispherical, and the dye jet is located just a few hundred microns from the HR flat. The jet was oriented normal to the laser axis. Several different dyes were used, and the best results were obtained with rhodamine 700 (also called LD 700). The output power and slope efficiency for this dye are shown in Fig. 9.3. Almost 400 mW of output power was achieved with a slope efficiency of 51%. The threshold pump power was 30 mW and the optical conversion efficiency was 50%.

The diode-pumped dye laser shown in Fig. 9.2 was operated with the diodes powered only with AA batteries, illustrating the high efficiency and convenience of this approach compared to ion laser pumping. The high stimulated emission coefficient, the facility with which the dye concentration can be adjusted for different pump wavelengths, and the use of angular multiplexing of multiple laser diodes for pump power scaling (the gain element is essentially two-dimensional) are all features that make dye lasers well suited for diode pumping. Clearly, diode pumping has important implications for applications requiring cw tunable near-IR dye laser emission.

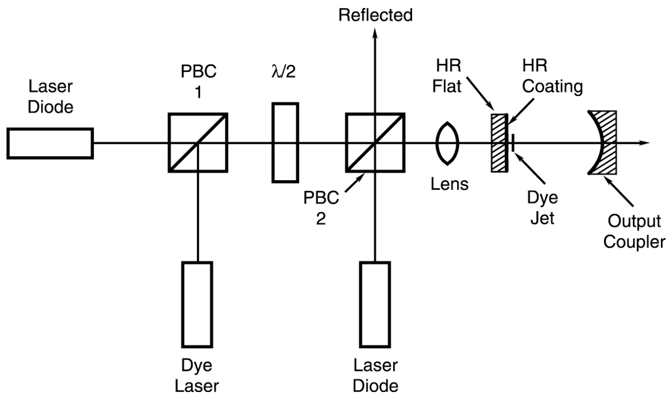

Figure 9.2. Arrangement of the pump and resonator optics for a diode-pumped dye laser.

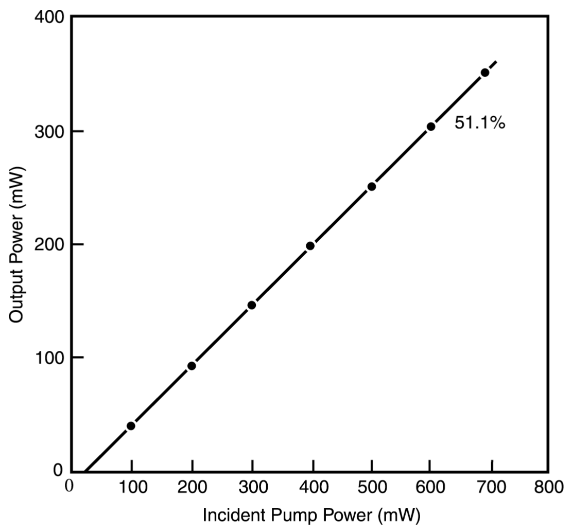

Figure 9.3. Pump power dependence of the rhodamine 700 dye laser.

Chapter 10

Intracavity Elements: Q-switching, SHG, and Single-Longitudinal-Mode Operation

In this chapter, three different types of diode-pumped laser operation are described. The first is repetitive *Q*-switching, which is useful for laser machining operations such as drilling or cutting, and is also used extensively in producing second harmonic generation (SHG). Intracavity cw SHG will also be reviewed. And finally, two techniques for producing diode-pumped single-longitudinal-mode laser output are explored.

10.1 Acousto-optic Q-switch for high repetition rate

When high-repetition-rate *Q*-switched output is desired, the standard technique involves pumping the rod with a cw source and using an acousto-optic (AO) *Q*-switch inside the resonator. *Q*-switching has been treated in numerous textbooks and will be described here only briefly.

A *Q*-switch is a shutter that is located inside the laser cavity. When the shutter is closed, feedback is prevented and no laser emission is produced. If the rod is pumped while the shutter is closed, the primary means by which energy is lost is through spontaneous emission. Therefore, if the pump is a pulsed source such as a flashlamp, the excitation pulse generally begins about 1 fluorescence lifetime (τ_f) prior to the opening of the *Q*-switch. Excitation with pulsed sources like flashlamps produce high peak energies under *Q*-switched operation.

This section addresses high-repetition-rate *Q*-switching. The rod is pumped continuously using cw laser diodes. The dynamics of repetitive *Q*-switching is, briefly stated, that at low repetition rates (where "low" and "high" repetition rates are referenced to $1/\tau_f$), the output energy per pulse is independent of *Q*-switch rate. Increasing the repetition rate increases the average output power. The pulse width stays more or less constant, at least to first order, so that the pulse peak power remains constant in this operating regime as well. The highest pulse energy E that can be produced with low-repetition-rate *Q*-switching and cw excitation is given by

$$E = P_{ss}\tau_f \,, \tag{10.1}$$

where P_{ss} is the maximum cw laser output power. For a 1-W Nd:YAG laser, E is 230 μJ. As can be seen from this equation, a longer fluorescence lifetime will produce a more energetic pulse, although at a lower repetition rate.

At a high repetition rate, the average power is constant, ideally equal to the cw output power P_{ss} (i.e., the laser power that would be obtained without the Q-switch). As the repetition rate increases in this regime, the energy per pulse drops, as does the peak power. In addition, as the pump excitation time for each pulse becomes significantly shorter than the upper-state lifetime, the upper-state population drops below the steady-state (low-repetition-rate) value. This reduces the gain and causes the pulse length to increase. Thus, the peak power drops more rapidly than it would if the energy per pulse were the only factor to be considered.

The temporal evolution of the upper laser level population density (n^*) is shown schematically in Fig. 10.1. Pumping is initiated at $t = 0$, and for pump pulse lengths $\tau_p \ll \tau_f$, the inversion density increases linearly with pulse length. This behavior is characteristic of high-repetition-rate (and therefore short-pump-pulse) operation. For $\tau_p \gg \tau_f$, the upper laser level population reaches steady state, where for the simplest case the pump rate P',

$$P' = \sigma_a I n_o / h\nu \,, \tag{10.2}$$

is equal to the spontaneous emission rate S, where

$$S = n^*/\tau_f \,, \tag{10.3}$$

and where σ_a is the absorption cross section, I is the pump intensity, and n_o is the dopant density. The steady-state upper laser level density n_{ss}^* is

$$n_{ss}^* = \sigma_a I n_o \tau_f \, / \, h\nu \tag{10.4}$$

and the curve shown in Fig. 10.1 is

$$n^* = n_{ss}^* (1 - e^{-t/\tau_f}). \tag{10.5}$$

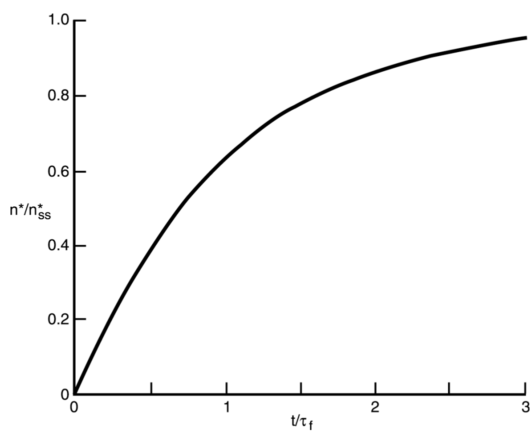

Figure 10.1. Temporal evolution of the upper-state population.

It can be seen from Fig. 10.1 that for the maximum energy out per pulse, the pump pulse width τ_p should be several times τ_f. However, pumping for times much longer than τ_f does not produce efficient *Q*-switched operation, since the incremental increase in n^* with additional pump pulse length diminishes as the curve begins to bend over. The highest efficiency will occur in the linear region of the curve, although the pulse energy is reduced and the pulse width increased relative to the case of longer pulse excitation. This is due to the lower gain. Therefore, a good compromise between high peak power and good efficiency is produced when $\tau_p \approx \tau_f$. Pulse lengths of this duration are typically used for low-repetition-rate flashlamp-pumped *Q*-switched lasers as well.

In Section 3.4.1 it was noted that the *Q*-switched pulse length depends inversely on the ratio ("*r*") of the resonator gain to the passive loss, and is expressed as a multiple of the cavity decay time. Note that the gain is directly proportional to n^*. For $r > \sim 10$ this "multiple" approaches 1, and the pulse length is determined by the cavity decay time.

An AO *Q*-switch is typically used for high-repetition-rate *Q*-switched operation. This switch contains a crystal such as quartz, and a diffraction grating is established in the crystal using acoustic waves. The grating operates in transmission mode and introduces loss by diffracting part of the resonant flux out of the feedback path. To properly utilize the grating, the resonator mode should be collimated as it passes through the *Q*-switch. Optical damage to the *Q*-switch can occur if the mode is focused at the acousto-optic crystal. In the past, commercially available *Q*-switches were relatively large devices, designed to handle high average powers for lamp-pumped lasers. In the last five years a newer line of miniature *Q*-switches has been developed. These are used in most commercial diode-pumped lasers, as they are compatible with the compact geometry and relatively low intracavity fluence of these devices.

10.2 Intracavity SHG for visible laser output

Most solid state lasers operate in the IR, while many applications require visible laser emission. Because of the numerous advantages of solid state lasers in general, and diode-pumped lasers in particular, there has been a strong motivation to produce all-solid-state visible lasers. A major step in this direction has been the utilization of second harmonic generation, which involves passing the fundamental wavelength through a second harmonic generating (SHG) crystal.

For cw lasers, the SHG crystal is generally located within the resonator cavity. The high fundamental intracavity flux increases the conversion efficiency (which increases as the square of the intensity). An alternative to intracavity SHG is to place the crystal outside the resonator in an external cavity, for example. This configuration requires single frequency radiation, and the external cavity must be tuned to resonate at the fundamental frequency. A simpler approach for external SHG involves the recently introduced periodically poled crystals such as periodically poled lithium niobate (PPLN). Periodically poled material is in its early stages of development.

The most commonly used SHG crystal for Nd-doped lasers operating at 1 μm is KTP, potassium titanyl phosphate. SHG produces laser output at 532 nm for Nd:YAG, and of course this wavelength will vary somewhat for other Nd host crystals. The doubling efficiency of KTP for diffraction-limited light focused to a minimum spot size over the length of the crystal is approximately 0.2% $W^{-1}cm^{-1}$. A 1-W cw laser would produce only 2 mW of 532-nm output through a 1-cm-long KTP crystal located external to the resonator. However, the intracavity flux might be 50 times as high as the emitted intensity. In this case, locating the 1-cm KTP crystal inside the cavity would produce 100 mW of 532-nm emission.

There are several considerations related to intracavity SHG that should be mentioned. First is the polarization. Whether Type I or Type II (KTP used for 532-nm SHG is Type II) SHG requires polarized input. Therefore, the orientation of the laser rod and SHG crystal axes should be properly aligned. In addition, depolarization effects such as thermal birefringence or rotation of the polarization by the SHG crystal (SHG crystals may act as thermally sensitive waveplates) will introduce losses.

The crystal should be located at a waist since the conversion efficiency depends on the square of the intensity. For end pumping, the laser rod is usually at the resonator waist. Therefore, the cavity mode must be designed to produce a second waist for the SHG crystal. Poynting vector walk-off must be factored into the resonator mode design. The solid angle of the focused beam should be less than the crystal acceptance angle.

Third, as was mentioned in Section 3.4.1, intracavity SHG has a tendency to produce amplitude noise in diode-pumped lasers. The noise is due to sum-frequency generation between different longitudinal modes. There are several approaches to eliminating this noise, including unidirectional rings, longer cavities, and the insertion of a quarter-wave plate. Many of the currently available commercial diode-pumped lasers do not exhibit amplitude noise.

10.3 Single-longitudinal-mode lasers

Single-longitudinal-mode (SLM) lasers, also called single-frequency lasers, oscillate on only one longitudinal mode and hence produce single-frequency output. One of the more interesting facets related to the development of diode-pumped lasers is the opportunity to produce certain types of lasers that are impractical to operate using conventional pumping techniques. SLM lasers are representative of this. In this section, the operation of two different types of SLM lasers are described. There are of course many other ways of building single-frequency lasers than the two described here.

It might be worthwhile to explain briefly why most lasers are not single mode. Most laser cavities generate standing waves having peaks and nodes. A standing wave at any given frequency will not extract gain where it has a node. This is called "spatial hole burning." A second frequency oscillating in the cavity may have amplitude peaks at some of the same locations along the resonator axis where the first frequency has nodes. If the gain for the second frequency exceeds the loss, it will oscillate simultaneously with the first. Furthermore, both frequencies may have nodes in certain other locations where the rod has gain, allowing a third frequency to oscillate. In general, multiple frequencies will oscillate simultaneously as long as the spatial distribution of the gain in the active volume of the resonator is such that the threshold condition is exceeded for each. This of course assumes that the laser transition is homogeneously broadened, meaning that any excited ion can produce laser emission at a given frequency within the gain bandwidth.

10.3.1 Ring lasers

If a laser is designed to support a traveling wave rather than a standing wave, then there is no spatial hole burning and a single longitudinal mode is produced. In a traveling wave, the nodes and peaks move continually along the resonator axis. The frequency experiencing the highest net gain (gain minus loss) depletes the inversion, so that it is the only longitudinal mode produced by the laser.

Lasers that support traveling waves are called “ring lasers.” In this type of laser, light makes a complete circuit along the resonator axis without retracing its path. However, ring lasers can also support standing waves since the light may propagate in both directions at the same time. Bidirectional oscillation produces spatial hole burning, and the resulting output is not single mode.

To produce unidirectional oscillation there must be higher loss for light propagating in one direction (e.g., counterclockwise) than in the other (clockwise). In the most general case this is accomplished with the use of a Faraday rotator, a half-wave plate, and a linear polarizer. The Faraday rotator rotates the beam polarization. The direction of the rotation is nonreciprocal, as it depends on the direction of propagation of the beam through the rotator. If the polarization of the counterclockwise beam is rotated in the counterclockwise direction, the polarization of the clockwise beam is rotated in the clockwise direction. The half-wave plate provides reciprocal polarization rotation; that is, it rotates the polarization in the same direction independent of the beam propagation direction through the plate. It is aligned to rotate the polarization of the clockwise beam back to its original orientation. In this example, it would provide rotation in the counterclockwise direction. At the same time, the half-wave plate rotates the counterclockwise beam even further away from its original polarization orientation. When the clockwise beam passes through the linear polarizer it suffers no loss, since the orientation of its polarization is restored by the half-wave plate. However, the polarizer introduces loss for the counterclockwise beam.

Providing unidirectional operation does not require large loss. Even a few hundredths of a percent of additional loss per pass will make the ring unidirectional. The unidirectional ring produces a single-longitudinal-mode output.

An efficient, diode-pumped ring laser is illustrated in Fig. 5.4. Referring back to that figure, it can be seen that all of the components required to produce unidirectional operation are in the resonator. The Faraday rotator is the Nd:YAG crystal. Nd:YAG has a high Verdet coefficient and is located inside a Nd-Fe-B high field magnet. This provides the nonreciprocal polarization rotation. The half-wave plate or birefringent tuner produces the appropriate reciprocal polarization rotation, canceling the rotation for the wave traveling in the clockwise direction. The linear polarizer is the Nd:YAG rod oriented at Brewster's angle.

The performance[10] of this device is excellent. Almost 500 mW was reported for a single-frequency mode with a pump power of less than 4 W. The measured linewidth was less than 1.5 MHz.

10.3.2 "Microchip" lasers

If the resonator length is short enough, only one frequency will be supported no matter how high the gain is at the nodes.[*] This is due to the free spectral range of the Fabry-Pérot resonator relative to the gain bandwidth of the laser crystal, and is the basis of the microchip laser. This laser is simple to align, supports a standing wave, and produces a single longitudinal mode. Numerous versions of this laser have been produced. For low-power operation these lasers are very useful, but for higher power the efficiency drops. This is because none of the gain at the spatial holes can be used.

Most microchip lasers are composed of flat-flat resonators. For these lasers the resonator mode is confined by gain guiding. Some microchip lasers have been developed in the shape of miniature lenses to provide better mode confinement and more stable operation. An example of one of these devices, which was packaged into a mount holding all of the optical components, is shown in Fig. 10.2. The entire laser is the monolithic lenslike structure in the figure (which is appropriately coated on both faces). This laser produced[11] approximately 30 mW single mode when diode pumped. Under higher-power diode pumping, the laser produced several simultaneous longitudinal modes with a total output power of just under 500 mW. The pump power used was 1.2 W.

[*] This is true up to a point, but when the pump intensity is high enough there will be sufficient gain at the wings of the gain curve to permit adjacent longitudinal modes to produce multimode output. The level of pump intensity required to produce multimode operation depends on th laser length and gain bandwidth of the materal. For very short cavaties, the pump intensity requirements are extremely high.

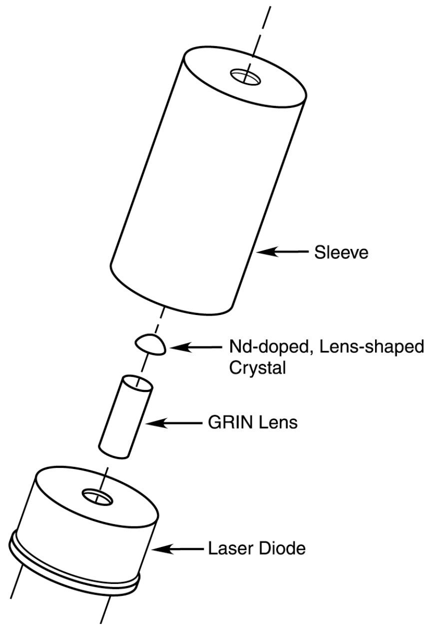

Figure 10.2. Exploded view of a single-frequency microchip laser, including the pump optics and housing.

Chapter 11

Conclusion

We have covered quite a bit of ground for an introductory text, and it will be of some benefit to briefly review the topics presented. We started by addressing the fundamentals of diode pumping. Concepts were presented that describe optical pumping, laser resonators, modes, and pump optics. We also described the emission features of laser diodes and diode arrays that are used as pump sources, addressing both the spatial and spectral properties. The importance of these concepts for understanding the fundamentals of diode-pumped solid state lasers was noted in several sections.

In the second part of the text we presented the detailed design of a 1-W cw TEM_{00} 1.06-μm laser. We put into practice the general concepts presented in the first part of the text, and described the rationale for selecting the pump optical components, the resonator configuration, coatings, diodes, and control electronics. We followed this by describing the operation of the laser we designed, particularly the gain and loss parameters, and the optimum output coupling. We then discussed the six efficiency factors that are involved in determining the overall or "wall plug" laser efficiency. By following the "trail of photons" from the pump diode emission to the 1.06-μm output, we are able to identify the parameters that affect overall laser efficiency.

In the third part of the text, we began by discussing the issues involved in power scaling. This was followed by (briefly) examining the concepts involved in side pumping, and describing the operation of two novel side-pumped resonators. We concluded the third part by providing a survey of numerous topics that are of current interest in diode-pumped laser development. We mentioned two other emission wavelengths produced by Nd-doped lasers, and indicated that pump wavelength bands generated by laser diodes other than AlGaAs are used for pumping various gain media. Three different diode-pumped lasers were mentioned, and the third part concluded by touching upon the operation of diode-pumped Nd lasers in modes such as repetitively *Q*-switched, intracavity second harmonic generation, and single frequency emission.

In an introductory text there is little opportunity to be thorough. This is particularly true when presenting such diverse topics as were considered in the third section. However, it is hoped that the reader has gained an overall perspective of this fascinating field, and will appreciate the interplay of the various optical parameters in terms of their overall impact on laser performance.

Bibliography

There are numerous basic texts on laser design and optical resonators. Some examples are

- *Lasers*, A.E. Siegman, University Science Books, Mill Valley, 1986.
- *Laser Electronics*, J. T. Verdeyen, Prentice-Hall, Englewood Cliffs, 1981.
- *The Physics and Technology of Laser Resonators*, D.R. Hall and P. E. Jackson, Eds., Adam Hilger, Bristol, 1989.
- *Solid-State Laser Engineering*, W. Koechner, Springer-Verlag, Berlin, 1988
- *Principles of Lasers*, O. Svelto, Plenum Press, 1998.

One of the most often-cited and comprehensive texts on laser crystals is

- *Laser Crystals*, A. A. Kaminskii, Springer-Verlag, Berlin, 1990.

Books providing useful information on nonlinear optics are

- *Nonlinear Optics*, P.G. Harper and B.S. Wherrett, Eds., Academic Press, London, 1977.
- *Handbook of Nonlinear Optical Crystals*, Springer-Verlag, Berlin, 1999.

References

1. D.R. Scifres, R.A. Sprague, W. Streifer and R.D. Burnham, “Focussing of a 7700-Å high power phased array semiconductor laser,” *Appl. Phys. Lett.*, **41**, p. 1121 (1982).
2. J. Berger, D.F. Welch, D.R. Scifres, W. Streifer and P.S. Cross, “370 mW, 1.06 μm, cw TEM00 output from an Nd:YAG laser rod end-pumped by a monolithic diode array,” *Electron. Lett.*,**23**, p.669 (1986).
3. See for example R. Scheps, “Efficient Cr,Nd:$Gd_3Sc_2Ga_3O_{12}$ laser at 1.06 μm pumped by visible laser diodes,” *Appl. Phys. Lett.*, **59**, p.1287 (1991).
4. K. Otsuka, T. Yamada, M. Saruwatasri and T. Kimura, *IEEE J. Quantum Electron.*, “Spectroscopy and laser oscillation properties of lithium neodymium tetraphosphate,” *IEEE J. Quantum Electron.*, **QE-11**, p. 330 (1975).
5. W.P. Risk, “Modeling of longitudinally pumped solid-state lasers exhibiting reabsorption loss,” *J. Opt. Soc. Am. B*, **5**, p. 1412 (1988).
6. P.F. Moulton, “An investigation of the Co:MgF_2 laser system,” *IEEE J. Quantum Electron.*, **QE-21**, p.1582 (1985).
7. R. Scheps, “Internally folded scalable laser,” U.S. Patent No. 5,249,196, September 28, 1993.
8. J.E. Bernard and A.J. Alcock, “High-efficiency diode-pumped Nd:YVO_4 slab laser,” *Opt. Lett.*, **18**, p. 968 (1993).
9. R. Scheps, “Near-IR dye laser for diode-pumped operation,” *IEEE J. Quantum Electron.*, **31**, p.126 (1995).
10. R. Scheps and J.F. Myers, “Scalable single frequency diode-pumped ring laser,” *Appl. Opt.*, **31**, p.1221 (1992).
11. R. Scheps and D.F. Heller, “Single mode operation of a standing wave miniature Nd laser pumped by laser diodes,” *Appl. Opt.*, **28**, p. 5288 (1989).

Index

About the Author

Richard Scheps has been developing diode-pumped lasers since 1986. He has published extensively in this field and was the first to demonstrate diode pumping in various gain media, including Cr:LiCAF, Cr,Nd:GSGG, and rhodamine 700 (LD700). He has served as Editor of the *IEEE Journal of Selected Topics in Quantum Electronics* and as an Associate Editor of *Photonics Technology Letters.* He is currently Associate Editor of the *IEEE Journal of Quantum Electronics* and Editor of *Progress in Quantum Electronics*. He holds more than 20 patents in the field of lasers and electro-optics.